Responses of field-grown maize to different soil types, water regimes, and contrasting vapor pressure deficit

Thuy Huu Nguyen[1], Thomas Gaiser[1], Jan Vanderborght[3], Andrea Schnepf[3], Felix Bauer[3], Anja Klotzsche[3], Lena Lärm[3], Hubert Hüging[1], Frank Ewert[1, 2]

[1]University of Bonn, Institute of Crop Science and Resource Conservation (INRES), Katzenburgweg 5, 53115 Bonn, Germany

[2]Leibniz Centre for Agricultural Landscape Research (ZALF), Institute of Landscape Systems Analysis, Eberswalder Strasse 84, 15374 Muencheberg, Germany

[3]Agrosphere (IBG-3), Institute of Bio- and Geosciences, Forschungszentrum Jülich GmbH, 52428, Jülich, Germany

*Corresponding author, email: tngu@uni-bonn.de

Abstracts

Drought is a serious constraint to crop growth and production of important staple crops such as maize. Improved understanding of the responses of crops to drought can be incorporated into cropping system models to support crop breeding, varietal selection and management decisions for minimizing negative impacts. We investigate the impacts of different soil types (stony and silty) and water regimes (irrigated and rainfed) on hydraulic linkages between soil and plant, as well as root: shoot growth characteristics. Our analysis is based on a comprehensive dataset measured along the soil-plant-atmosphere pathway at field scale in two growing seasons (2017, 2018) with contrasting climatic conditions (low and high VPD). Roots were observed mostly in the topsoil (10-20 cm) of the stony soil while more roots were found in the subsoil (60-80 cm) of the silty soil. The difference in root length was pronounced at silking and harvest between the soil types. Total root length was 2.5 - 6 times higher in the silty soil compared to the stony soil with the same water treatment. At silking time, the ratios of root length to shoot biomass in the rainfed

plot of the silty soil (F2P2) were 3 times higher than those in the irrigated silty soil (F2P3) while the ratio was similar for two water treatments in the stony soil. With the same water treatment, the ratios of root length to shoot biomass of silty soil was higher than stony soil. The seasonally observed minimum leaf water potential (ψ_{leaf}) varied from around -1.5 MPa in the rainfed plot in 2017 to around -2.5 MPa in the same plot of the stony soil in 2018. In the rainfed plot, the mimimum ψ_{leaf} in the stony soil was lower than in silty soil from -2 to -1.5 MPa in 2017, respectively while these were from -2.5 to -2 MPa in 2018, respectively. Leaf water potential, water potential gradients from soil to plant roots, plant hydraulic conductance (K_{soil_plant}), stomatal conductance, transpiration, and photosynthesis were considerably modulated by the soil water content and the conductivity of the rhizosphere. When the stony soil and silt soil are compared, the higher 'stress' due to the lower water availability in the stony soil resulted in less roots with a higher root tissue conductance in the soil with more stress. When comparing the rainfed with the irrigated plot in the silty soil, the higher stress in the rainfed soil resulted in more roots with a lower root tissue conductance in the treatment with more stress. This illustrates that the 'response' to stress can be completely opposite depending on conditions or treatments that lead to the differences in stress that are compared. To respond to water deficit, maize had higher water uptake rate per unit root length and higher root segment conductance in the stony soil than in the silty soil, while the crop reduced transpired water via reduced aboveground plant size. Future improvements of soil-crop models in simulating gas exchange and crop growth should further emphasize the role of soil textures on stomatal function, dynamic root growth, and plant hydraulic system together with aboveground leaf area adjustments.

Key words: irrigation, plant hydraulic conductance, transpiration, root length, soil types, soil to leaf water potential, stomatal regulation

Abbreviations: DOY: day of the year; DAS: day after sowing; TUE: transpiration use efficiency; SF: sap flow; LAI: green leaf area index; PAR: photosynthetically active radiation; VPD: vapor pressure deficit; An: net leaf photosynthesis; E: leaf transpiration; ψ_{leaf}: leaf water potential; $\psi_{sunlitleaf}$: leaf water potential of sunlit

leaf; $\psi_{shadedleaf}$: leaf water potential of shaded leaf; K_{soil}: hydraulic conductance of soil; K_{root}: root hydraulic conductance; K_{stem}: stem hydraulic conductance; ψ_{soil_effec}: effective soil water potential; $\psi_{difference}$: difference between effective soil water potential and sunlit leaf water potential; K_{soil_root}: root system hydraulic conductance (includes soil and root hydraulic conductance); K_{soil_plant}: whole plant hydraulic conductance (includes below and aboveground components).

1. Introduction

Maize (*Zea mays L.*) is a major staple crop throughout the world. Drought stress, which negatively affects crop growth and yield, is of increasing concern in several important maize cultivating regions (Daryanto et al., 2016). Increases in frequency and severity of drought events due to climate change have been recently reported (IPCC, 2022). Thus, field observations and understanding on how maize responds to water stress are necessary to suggest promising traits for breeding programs (Vadez et al., 2021) as well as irrigation schemes (Fang and Su, 2019; Q. Cai et al., 2017). Improved understanding of crops' response to drought can be incorporated into soil-crop models (e.g. crop modelling and soil-vegetation-atmosphere transfer modelling).

Stomatal regulation is often considered as a key aboveground hydraulic variable in regulating water use of crops. Maize is known as an isohydric plant. Maize stomata are closed in response to drought conditions to maintain leaf water potential (ψ_{leaf}) above critical levels ($\psi_{threshold}$ or minimum ψ_{leaf}) (Tardieu and Simonneau, 1998). The isohydric behavior is due to different mechanisms including hydraulic and/or chemical (e.g. abscisic acid [ABA]) signals (Tardieu, 2016). The degree to which these underlying mechanisms interact and differ among genotypes and/or environmental scenarios in explaining the stomatal regulation is still debated (Tardieu, 2016, Hochberg et al., 2018). Field evidence in variation of the minimum ψ_{leaf} of maize due to soil water availability and soil hydraulics is rarely reported.

Water flow along the soil-plant-atmosphere continuum is determined by a series of hydraulic conductivities and gradients in water potential. Hydraulic conductance of soil (K_{soil}), root hydraulic

conductance (K_{root}), and stem hydraulic conductance (K_{stem}) determine water potential from soil to root and root xylem water, and thus magnitude of ψ_{leaf}. There are two main resistances to water flow from the soil to the shoot, namely the soil and the root resistances, often expressed as their inverse, K_{soil} and K_{root} (Nguyen et al., 2020; Cai et al., 2018). In wet soils, the soil hydraulic conductivity is much higher than that of roots, and water flow is mainly controlled by root hydraulic conductivity (Hopmans and Bristow, 2002; Draye et al., 2010). It is well-known that a decrease in soil matric potential and soil hydraulic conductivity triggers stomatal closure and thus results in reduction in transpiration rate (Sinclair and Ludlow, 1986; Carminati and Javaux 2020; Abdalla et al., 2021). For the root water uptake and controlling stomata, the location where soil and roots are in close contact (rhizosphere) is most important, because when this thin layer of rhizosphere is disconnected (i.e. soil-root contact is lost), the water movement from soil toward the roots is reduced, which might trigger stomatal closure to maintain hydraulic integrity of plant (Carminati et al., 2016; Rodriguez-Dominguez and Brodribb, 2019; Abdalla et al., 2022). The magnitude of the drop of water potential between bulk soil and soil-root interface increases considerably at different levels of soil dryness for different soil types (Carminati and Javaux, 2020; Abdalla et al., 2022). Hydraulic limits in the soil (Carminati and Javaux, 2020), or in the root–soil interface [as measured for olive trees by Rodriguez-Dominguez and Brodribb, 2019 or tomato (Abdalla et al., 2022)], or in the root properties (Bourbia et al., 2021; Cai et al., 2022; Nguyen et al., 2020; Cai et al., 2018) or due to both soil textures and root phenotypes (Cai et al., 2022b) emphasized the importance of belowground hydraulics (Carminati and Javaux, 2020). However, also the shoot hydraulic conductance could be limiting in some crop plants (Gallardo et al., 1996) or in trees (Domec and Pruyn, 2008; Tsuda and Tyree, 1997). Stomatal conductance and shoot hydraulic conductance showed close links to each other in pine trees (Hubbard et al., 2001). This summary illustrates three points: (i) current studies have often focused either on above or on below hydraulic limits, but rarely consider both (ii) the roles and relations of soil hydraulic properties to root and plant hydraulic conductance (thus influences on stomatal conductance) remain unclear (iii) the role of

different hydraulic processes across the soil - plant - atmosphere continuum i.e. soil to roots, stem, and soil-plant hydraulic conductance in controlling stomatal conductance remains unclear.

Simultaneous measurements of atmospheric conditions (light intensity and vapor pressure deficit), leaf water potential, and transpiration rates, coupled with measurements of root, stem and whole soil-plant hydraulic conductance, root architecture, and soil water potential distribution could reveal the relative importance of rhizosphere, shoot and root growth, and hydraulic conductance vulnerability, especially under progressive soil drying at field conditions (Carminati and Javaux, 2020; Tardieu et al., 2017). For the soil water conditions, soil texture and hydraulic characteristics are very important because they influence soil water movement and thus affect infiltration, surface and sub-surface runoff, and ultimately plant available soil water (Vereecken et al., 2016). Soil texture properties, characterized by different fractions of clay, silt, and sand particles, are important drivers in determining the soil water retention properties (Scharwies and Dinneny, 2019; Stadler et al., 2015; Zhuang et al., 2001). Soil with higher water holding capacity (here the silty soil with low stone content) have a larger amount of plant available water which in turn enables crops to better meet the evaporative demand and facilitates better crop growth as compared to the soil with high stone content (Nguyen et al., 2020; Cai et al., 2018). Estimations of hydraulic conductance (different organs and whole plant hydraulic conductance) were done for crop plants and maize mainly under controlled environment or pot conditions e.g. for different species and genotypes during soil drying (Sunita et al., 2014; Choudhary and Sinclair, 2014; Abdalla et al., 2022; Meunier et al., 2018; Wang et al., 2017; Li et al., 2016) or various species and genotypes together with different soil textures (Cai et al., 2022a), or soil texture with different vapor pressure deficit (VPD) (Cai et al., 2022b). Compared to the substantial effect of soil texture, there was no evidence of an effect of VPD on both soil–plant hydraulic conductance and on the relation between canopy stomatal conductance and soil–plant hydraulic conductance in pot-grown maize (Cai et al., 2022b). Contrast results were found in winter wheat where plant hydraulic conductance increased with rising VPD for some genotypes in wet conditions

(Ranawana et al., 2021). Vadez et al., (2021) examined the effects of soil types together with increasing VPD on transpiration efficiency (TE) and yield under pot conditions for several C_4 species (maize, sorghum, and millet). The interpretation of differences in TE was attributed to soil types, more specifically, to the differences in soil hydraulic properties and soil hydraulic conductance. However, experimental evidence linking root hydraulics to stomatal regulation was lacking in these two Vadez's studies (Vadez et al., 2021). Recent field studies have aimed at quantification of root hydraulic conductance and it's linkages with crop growth (leaf area and biomass) under different soil types (in wheat Cai et al., 2017; Cai et al., 2018; Nguyen et al., 2020 or maize in Nguyen et al., 2022; Jorda et al., 2022). However, field studies that consider both below (soil-root hydraulic conductance) and above (stem hydraulic conductance), or soil-plant hydraulic conductance (including below and above-ground parts) and their roles in stomatal regulation as well as crop growth (leaf area and biomass) are rarely carried out.

This study aims at further understanding of the hydraulic linkages between soil and plant and responses of plants to drought stress in relation to root: shoot growth characteristics at field scale. We hypothesize that, in field-grown maize, (1) soil-plant hydraulic conductance depends on soil hydraulic properties, especially under dry soil conditions (2) minimum leaf water potential of maize is similar across soil types, water treatments and climatic conditions. The hypotheses will be tested through three objectives: (i) to investigate the effects of soil types, water application, and climatic condition on root growth and (ii) on stomatal conductance, leaf photosynthesis, transpiration, leaf water potential, different components of the hydraulic conductance (root, stem, and whole soil-plant), and (iii) to analyze the relative contribution of root and shoot growth (leaf area and biomass) on the water uptake capacity of maize. These three objectives will be achieved based on a comprehensive dataset covering the whole soil-plant continuum over two growing maize seasons with contrasting climatic conditions (low and high VPD) under two water treatments (rainfed and irrigated) and two different soil types (stony and silty soil).

2. Materials and methods

2.1. Location and experimental set-up

We carried out a field experiment at two rhizotron facilities in Selhausen, North Rhine-Westphalia, Germany (50°52'N, 6°27'E). The field is slightly inclined with a maximum slope of around 4. One rhizotrone facility was located upslope (F1) with around 60% gravel by weight in the 10-cm topsoil while the second rhizotrone facility was at downslope (F2) with silty soil (stone content is around 4% by weight).

Each rhizotrone facility was divided into three subplots of 7.25 m by 3.25 m: two rainfed plots (P1, P2), and one irrigated plot (P3). In rainfed plots P1, other sowing densities and dates were used than in the other plots and we excluded therefore these plots. Silage maize *cv.* Zoey was sown on 4 May and 8 May in 2017 and 2018, respectively, with a plant density of 10.66 seeds m^{-2} (Figure 1a; Table 1). Detailed information of crop management practices is provided in Table 1.

[Insert Table 1 here]

2.2. Water applications

The irrigation systems [T-Tape 520-20-500 drip lines (Wurzelwasser GbR, Müzenberg, Germany)] were installed parallel to the crop rows with 0.3 m intervals. A nearby weather station (approx. 100 m from the experiment) recorded every 10 minutes weather variables (global radiation, temperature, relative humidity, precipitation, and wind speed). In addition, the precipitation amount was manually collected by a plastic rain gauge next to each rhizotrone facility. The Penman-Monteith equation was employed to estimate reference evapotranspiration. Daily crop evapotranspiration was calculated based on the single crop coefficient and the reference evapotranspiration (Allen et al., 1998). Irrigation amounts were estimated as the weekly sum of the calculated crop evapotranspiration. A total amount of 230 mm precipitation was recorded during the growing period (136 days) while average, minimum and maximum daily air temperature were 17.6, 8.3, and 25.3 °C, respectively (Fig. 1b). The crop on the irrigated plots (2017F1P3 and 2017F2P3) was received in total 130 mm (10 times, every 5-7 days, using 13 mm of

irrigation water per event) between mid June to end of August (Fig. 1b). Average, minimum, and maximum daily air temperature in 2018 were higher than in 2017 with 19.2, 10.85, and 27.3 °C, respectively (Fig. 1b). The summer season in 2018 could be considered as an extreme year with respect to plant growth at our experimental location due to exceptionally hot and dry weather conditions. Crop received only 91.3 mm of rain during the growing period of 2018 (107 days). The crop on the irrigated plots 2018F1P3 and 2018F2P3 was irrigated every 5-7 days (in total 13 times), with a total amount of irrigation of 257 mm and 239 mm between mid- June and mid- August, respectively (Fig. 1d). To avoid a crop failure due to severe drought in 2018, the rainfed plot in the stony soil (2018F1P2) had to be irrigated (in total 66 mm) four times (using 13, 22, 13, and 18 mm, respectively) (Fig. 1d). Detailed estimates of irrigation amount and intervals could be found in Nguyen et al., (2022a).

[Insert Figure 1 here]

2.3. Measurements

2.3.1. Soil water measurement and root growth

MPS-2 matrix water potential and temperature sensors (Decagon Devices Inc., UMS GmbH München, Germany) were installed at soil depths of 10, 20, 40, 60, 80, and 120 cm to measure half-hourly soil water potential and soil temperature. The range of the water potential measurements is from -9 kPa to approximately -100000 kPa (pF 1.96 to pF 6.01). In addition to MPS-2, soil water potential was measured by pressure transducer tensiometers (T4e, UMS GmbH, München, Germany) where the minimum detectable suction is -85 kPa to +100 kPa. A detailed description of sensor installation, calibration and data post processing can be found in Cai et al., (2016).

Minirhizotubes (7 m long clear acrylic glass tubes with outer and inner diameters of 6.4 and 5.6 cm, respectively) were installed horizontally at six different depths of 10, 20, 40, 60, 80, and 120 cm below the soil surface in each facility. There are three replicate tubes at each depth, accounting for 54 tubes in each

facility. Root measurements were taken manually by Bartz camera (Bartz Technology Corporation) (23 June 2017 – 12 September2017) and VSI camera (Vienna Scientific Instruments GmbH) (08 June 2017 – 22 June 2017) in 2017 while only VSI was used in 2018 (23 May2018 - 23 August 2018). Root images were taken at 20 fixed positions from the left- and right-hand sides of each tube weekly (or biweekly) during the growing seasons. The root images were analyzed by automated minirhizotube image analysis pipeline for segmentation and automated feature extraction (Bauer et al., 2021). Two-dimensional root length density (RLD, in units of cm cm^{-2}) was estimated from the total root length observed in the image and the image surface area. The overview of camera system, minirhizotube images acquisition, and post-processing of the root data were described in detail in Bauer et al. (2021) and Lärm et al., (2023).

2.3.2. Crop growth, leaf gas exchange, leaf water potential, and sap flow measurements

The phenology, plant height, stem diameter, green and brown leaf area, dry matter of different organs, and total aboveground dry matter were observed and measured bi-weekly. Dates of sowing, emergence, tasseling, and silking for two growing seasons were observed. There was difference in emergence, tasseling and silking dates for two growing seasons due to the differences of sowing dates and temperature. However, the developmental stages were not different among water treatments and soil types within one season. Measurements of green leaf area and aboveground dry matter were based on the destructive method.

We performed leaf gas measurements under clear sky and sunny conditions. Hourly leaf stomatal conductance (Gs), net photosynthesis (An), and leaf transpiration (E) of two sunlit leaves (uppermost fully developed leaves) and one shaded leaf of different plants were measured every two weeks. The Gs, An, and E were measured at steady-state using a LICOR 6400 XT device (Licor Biosciences, Lincoln, Nebraska, USA). Leaf water potential (ψ_{leaf}) was measured with a pressure chamber (SKPM 140/ (40-50-80), Skye Instrument Ltd, UK).

Based on stem diameter size, twenty sap flow sensors (SGA 13, SGB 16, and SGB 19 types) were installed (one sensor per plant and 5 maize plants per treatment) in each year. The sensors were operated from 7 July 2017 and from 28 June 2018 until harvest for the 2017 and 2018 growing season, respectively. The calculated sap flow in the plant (g h^{-1}) from the data loggers (Dynamax, 2007) was used to compute canopy transpiration based on the plant density per square meter. Further detail of developmental stages, crop growth, leaf gas exchange, leaf water potential, and sap flow measurements could be found in Nguyen et al., (2024), Nguyen et al., (2022a) and Nguyen et al., (2020).

2.4. Calculation of total root length, root system conductance, stem, and whole plant hydraulic conductance

To estimate the total root length from minirhizotubes, we adopted the option 2 which was described in Cai et al., (2017). Total root length per square meter soil surface area within each soil layer (m m^{-2}) was computed by multiplying the root length density with the corresponding soil layer thickness. The root length density was determined in each depth by dividing the measured root length per minirhizotron image by the assumed volume the roots would have occupied in absence of the tube, i.e., W * L * tube radius (see Cai et al., 2017).

Following Nguyen et al., (2020), the effective soil water potential was calculated based on hourly measured soil water potential (ψ_i) and normalized root length density at six depths (10, 20, 40, 60, 80, and 120 cm) ($NRLD_i$), and soil layer thickness (Δz_i) in the soil profile (Equation 1).

$$\psi_{soil\_effec} = \sum_{i=1}^{N} \psi_i NRLD_i \, \Delta z_i \quad (1)$$

We followed Ohm's law analogy by dividing the hourly sap flow by the difference between effective soil water potential and shaded leaf water potential to estimate root system conductance (K_{soil_root} - Equation 2), between shaded leaf water potential and sunlit leaf water potential to estimate stem hydraulic

conductance (K_{stem} - Equation 3), and between effective soil water potential and sunlit leaf water potential to estimate whole plant hydraulic conductance (K_{soil_plant} - Equation 4).

$$K_{soil\_root} = Sapflow/(\psi_{soil\_effec} - \psi_{shadedleaf}) \quad (2)$$

$$K_{stem} = Sapflow/(\psi_{shadedleaf} - \psi_{sunlitleaf}) \quad (3)$$

$$K_{soil\_plant} = Sapflow/(\psi_{soil\_effec} - \psi_{sunlitleaf}) \quad (4)$$

During one measurement day, four values of the K_{soil_root}, K_{stem}, and K_{soil_plant} were obtained from measurements between 11AM and 2 PM. The average and standard deviation of these hourly measurements were calculated for each measurement day in order to present the seasonal dynamics of those variables. To capture the diurnal and seasonal variations of sap flow and sunlit leaf water potential, in addition, we plotted the hourly sap flow and hourly difference of effective soil water potential and sunlit leaf water potential for three measurement days starting from predawn and whole seasons, respectively, to derive the slope which is also K_{soil_plant}.

2.5. Statistical analysis

Regression analysis was performed to understand the relationship between the sap flow volume and the difference of effective soil water potential and sunlit leaf water potential as well as the relationship between the total aboveground biomass and cumulated water transpired (sap flow volume). These analyses allow to derive the slope as proxy of K_{soil_plant} and transpiration use efficiency, respectively. Since all measured data have their own measurement errors, the generalized Deming regression was employed. We performed relationships (via correlation coefficient and statistical significant levels) of midday leaf An, Gs, and E with midday K_{stem}, K_{soil_plant}, K_{soil_root}, sunlit leaf potential, ψ_{soil_effec}, and the difference of ψ_{soil_effec} and sunlit leaf water potential ($\psi_{difference}$). All data processing and analysis were conducted using the R statistical software (R Core Team, 2022).

3. Results

3.1. Root growth under different water treatments, soil types and climatic conditions

Observed root length (cm cm^{-2}) from the minirhizotubes in different soil depths at the first week of June (stem elongation), around silking, and at harvest in two growing seasons are shown in the Figure 2. Root length was similar among water treatments at the start of stem elongation in both years (Fig. 2a & 2d). The difference in root length was pronounced at silking and harvest between the soil types. More root growth was observed in the silty soil compared to the stony soil with the same water treatment (i.e. 2.5 - 6 times higher at depth 40 cm). This indicated the strong negative effects of stone content on root development. In the stony soil, root length in the irrigated plot (F1P3) was slightly higher than in the rainfed plot (F1P2). In contrast, the rainfed treatment (F2P2) in the silty soil showed much higher root length, especially from 40 to 120 cm depths as compared to the irrigated plot (F2P3) in both growing seasons. Much lower stone content and deep soil cracks in the silty soil (Morandage et al., 2021) allow root extension to the subsoil, particularly in the rainfed plot F2P2. Root length in the rainfed treatment (F2P2) in 2018, is higher than in 2017 which implies that root further developed to exploit the water in the soil under the rainfed condition to meet the higher evaporative demand.

[Insert Figure 2 here]

Total root length (m m^{-2}) estimated from minirhizotubes and its ratio to shoot dry matter (m kg^{-1}) at three measured dates (as in Figure 2) are shown in the Figure 3. Total root length was much higher for the silty plots as compared to stony plots. In 2017, the highest total root length was observed in the rainfed plot of the silty soil (F2P2) with approximately 9166 m m^{-2} and 9878 m m^{-2} around silking and harvest, respectively, which was almost two times higher than in the irrigated plot (F2P3). These figures were higher in 2018 than 2017 where total root length of F2P2 was 10188 m m^{-2} and 13750 m m^{-2} at silking and harvest time, respectively. For the rainfed stony soil (F1P2), soil water depletion around the beginning of June in 2017 (Figure S1a) and from the first two weeks of June to harvest in 2018 (Figure S2a) caused the strong reduction of shoot biomass. In the stony soil, the shoot dry matter of the irrigated plot (F1P3) and the

rainfed plot (F1P2) were 1275 and 536 g m^{-2} at silking time (e.g. 19 July 2018 – DOY 200, Figure S3a and S3b). However, there was a minor difference between F1P2 and F1P3 in terms of the ratio of root length to shoot dry matter. In the silty soil, a decrease of soil water potential was not pronounced (compared to stony soil) in both years 2017 and 2018 (Figure S1b and S2b). In 2018, shoot biomass in the irrigated stony soil (F1P3) and silt soil (F2P3) were similar (1275 and 1299 g m^{-2}, respectively on 19 July 2018 – DOY 200) while the shoot biomass of the rainfed silty soil (F2P2) was 876 g m^{-2} (Figure S3a & S3b). However, the ratios of root length to shoot biomass in the rainfed plot of the silty soil (F2P2) were 3 and 6 times higher than those in the irrigated silty soil (F2P3) and stony soil (F1P3), respectively (e.g. 18 July, DOY 199). Moreover, total root length was relatively equal among treatments at the start of set elongation (8 June - DOY 159) in both years, while this was the opposite for the ratio of root length to shoot dry matter. This firstly illustrated that the finer soil texture without stones and with soil cracks could favor the root growth which indicates strong interactions of root and soil conditions. Secondly, the larger root length and higher atmospheric evaporative demand in 2018 than 2017 indicates also the interaction of root growth and climatic conditions.

[Insert Figure 3 here]

3.2. Stomatal conductance, photosynthesis, transpiration, and K_{soil_plant}

3.2.1. Diurnal course of stomatal conductance, photosynthesis, transpiration, and water potential at leaf level

After a long period with high temperatures and no rainfall, soil water reduction in the rainfed plot of the stony soil (F1P2) on 17 July 2018 (Figure S2) resulted in three times lower net photosynthesis (An), stomatal conductance (Gs), transpiration (E) and leaf water potential (ψ_{leaf}) as compared to the remaining treatments (Figure S4). This indicates that the soil water content strongly affected the stomatal conductance. Stomatal closure was much pronounced around midday in F1P2 while this was not the case in the F2P2, indicating the soil type strongly affected the stomatal conductance and leaf gas exchange.

Leaf gas exchange and leaf water potential in the F1P2 were still much lower than in other plots (Figure 4). On 18 July 2018, after application of 22.75 mm of irrigation water (at 4 PM), photosynthesis, stomatal conductance, transpiration and leaf water potential were slightly increased in F1P2. However, these were still smaller than in F2P2 and the two irrigated plots.

[Insert Figure 4 here]

On the next day after irrigation, leaf gas exchange and water potential were considerably increased in the F1P2 (Figure S5). Leaf curling was also less pronounced as compared the two previous days. Predawn and midday leaf water potential were around -0.4 MPa and -1.6 MPa for all plots, respectively. Leaf transpiration rate was around 3.1 millimole m^{-2} s^{-1} for all water treatments and soil types at 12 AM. This indicated the recovery of plant after watering at the rainfed plot with stony soil (F1P2).

3.2.2. Seasonal course of stomatal conductance, photosynthesis, transpiration, water potential, and plant hydraulic conductance at the leaf level

Seasonal stomatal conductance (Gs) and leaf water potential (ψ_{leaf}) are described in Figure 5. The relationship between two variables was rather noisy and non-linear. The leaf water potential showed distinct patterns among treatments in one growing season. Minimum ψ_{leaf} was maintained at around -1.5 MPa in the irrigated plot in stony soil (F1P3) and two plots in the silty soil (F2P2 and F2P3). Lower minimum ψ_{leaf} could be observed in the rainfed plot with stony soil (F1P2) but it did not go beyond -2 MPa. Minor leaf curling was observed only in the second week of June in the F1P2 in 2017. In 2018, the higher temperature and vapor pressure deficit resulted in lower minimum ψ_{leaf} in all treatments and soil types as compared to 2017. The minimum ψ_{leaf} was around -2 MPa in F1P3, F2P2, and F2P3 while ψ_{leaf} could drop below -2 MPa in F1P2 which was due to the severe soil water deficit. The low Gs and ψ_{leaf} associated with measurement dates when the substantial leaf curling was observed at mid of July to the end of growing season in F1P2 in 2018 (Figure S3c & S3d and Figure S6c & d).

[Insert Figure 5 here]

The effective soil water potential ($\psi_{soil\_effect\ MD}$), sunlit leaf water potential ($\psi_{sunlitleaf\ MD}$), stomatal conductance (Gs_{MD}), and whole plant hydraulic conductance ($K_{soil\_plant\ MD}$) at midday at several times during the growing season are presented in Figures 6 and 7 for 2017 and 2018, respectively. As expected, there was not much difference in terms of $\psi_{soil\_effecMD}$ among F1P3, F2P2, and F2P3 from 02 August to one week before harvest in 2017. The lowest $\psi_{soil\_effec\ MD}$ was observed in the F1P2. Leaf water potential dropped drastically but also $K_{soil\_plant\ MD}$ increased strongly whereas $\psi_{soil\_effec\ MD}$ remained quite similar (e.g. 18 July). This is because sap flow have increased substantially in this day (e.g. from 2.34 mm d^{-1} on 17 July to 6.97 mm d^{-1} on 18 July for the F1P2). The stomatal conductance decreased a lot in this day which could be explained that the atmospheric demand increased (e.g. global radiation was 13.6 MJ m^{-2} on 17 July compared to 23.9 MJ on 18 July while daily VPD was 0.7 kPa and 1.2 kPa, respectively) even more than the sap flow. Midday sunlit leaf water potential was not distinctively different among treatments with the lowest $\psi_{sunlitleaf\ MD}$ around -1.6 MPa throughout season. Also, Gs_{MD} was rather similar among plots. The $K_{soil\_plant\ MD}$ ranged from 0.125 to 0.96 mm h^{-1} MPa^{-1} with a sharp reduction before harvest. In general, the lowest values of $K_{soil\_plant\ MD}$ were found in F1P2 which was consistent with the smaller overall seasonal K_{soil_plant} (as the slope of linear relationship between sap flow and difference of effective soil water potential and sunlit leaf water potential) (see Figure S7).

[Insert Figure 6 here]

The $\psi_{soil\_effec\ MD}$ was substantially different in the two soil types and water treatments in 2018 (Figure 7a). Both F1P2 and F1P3 showed a gradual drop of $\psi_{soil\_effec\ MD}$ from 15 June until the third week of July then increased after irrigation events on 18 July (Figure S2b). However, $\psi_{soil\_effec\ MD}$ of F1P2 was much lower than F1P3 toward the harvest. The $\psi_{soil\_effec\ MD}$ of F2P2 and F2P3 only decreased progressively from around 10 July till harvest even though there was water supply from the irrigation (Figure S2b). The water applied by

irrigation and coming in by rainfall were insufficient to wet up the deeper soil layers which remained dry. The low Gs_{MD} was corresponding to the lowest $\psi_{sunlitleaf\ MD}$ and $K_{soil\_plant\ MD}$ from the F1P2 (Figure 7c & 7d). The $K_{soil\_plant\ MD}$ from all plots was ranging from 0.12 to 0.91 mm h^{-1} MPa^{-1}.There was the drop in $K_{soil\_plant\ MD}$ (i.e. 3 to 9 July or 17-18 July) before irrigation in this plot. However, it increased after the irrigation (i.e. 10 July and 19 July). This suggests that K_{soil_plant} depends strongly on the soil water content and the conductivity of the rhizosphere.

[Insert Figure 7 here]

3.2.3. Relationships of stomatal conductance, transpiration, photosynthesis with plant hydraulic variables at the plant canopy level

The slope of linear relationship between sap flow and difference of ψ_{soil_effec} and $\psi_{sunlitleaf}$ is shown for three consecutive days (leaf water potential measurements from the predawn) and before and after irrigation applications (17, 18, and 19 July 2018) (Figure 8). On both dates 17 and 18 July, the difference between ψ_{soil_effec} and $\psi_{sunlitleaf}$ was around -1.6 MPa with very low transpiration rates in the treatment F1P2 which was associated with very low plant hydraulic conductance and leaf curling. The whole plant hydraulic conductance was disrupted on these two days (0.06 and 0.16 mm h^{-1} MPa^{-1} for 17 and 18 July, respectively). Water was supplied on 18 July at 1 PM for the irrigated plots (F1P3, F2P3) as well as F1P2 at 4 PM (for saving plant from death due to severe drought stress). K_{soil_plant} was slightly changed (0.43 and 0.57 mm h^{-1} MPa^{-1} for F1P3 on 18 and 19 July, respectively and 0.5 and 0.58 mm h^{-1} MPa^{-1} for F2P3 on 18 and 19 July, respectively). However, the increase of K_{soil_plant} was substantial in the F1P2 after the irrigation. Soil water replenishment and an increase in the root - soil contact (Fig. 7a) allowed the K_{soil_plant} to recover overnight to 0.46 mm h^{-1} MPa^{-1}. This resulted in a narrower water potential gradient between root zone and sunlit leaf and in a higher transpiration rate on 19 July.

[Insert Figure 8 here]

373 Seasonal average of different midday hydraulic conductance components (root system hydraulic
374 conductance - K_{soil_root}, stem hydraulic conductance – K_{stem}, and whole plant hydraulic conductance –
375 K_{soil_plant}) are shown in Figure 9. In the same year, the K_{stem} was not much different among F1P3, F2P2, and
376 F2P3 plots. The K_{stem} of those plots was slightly higher than in the F1P2 in both years. In general, the K_{soil_root}
377 was lower than the K_{stem}. Overall, the estimated K_{soil_plant} was around 1/ ($1/K_{soil\_root}$ +$1/K_{stem}$) regardless of
378 soil types, years, and water treatments. The K_{soil_root} and K_{soil_plant} in the F1P2 in 2018 was much lower than
379 the remaining plots while the K_{soil_root} and K_{soil_plant} were not much different among plots in 2017. Our results
380 indicated that there was an impact of soil hydraulic conductance on K_{soil_root} and K_{soil_plant}. Although there is
381 a large difference in total root length between the two soil types (e.g. F1P3 versus F2P2 or F2P3 versus
382 F2P2), K_{soil_root} and K_{soil_plant} in those two plots were not much different. This could be explained by the fact
383 that K_{soil_plant} was not only depended on root length but also depended on the variability of root segment
384 hydraulic conductance.

385 [Insert Figure 9 here]

386 **3.3. Relative importance of root and leaf area growth to transpiration and crop performance at canopy**
387 **level**

388 Drought stress was observed in the rainfed plot (F2P2) in the second week of June 2017 with mild leaf
389 rolling. The crop then recovered due to sufficient rainfall and lower evaporative demand. Drought stress
390 occurring again at the stem elongation phase caused reduction of plant size (height and stem diameter)
391 (Figure S6) as well as a slight reduction of leaf area and biomass in this plot (Figure S3a & S3c). Transpiration
392 per unit of leaf area did not differ much among water treatments and soil types in 2017 (Figure S8). The
393 opposite was the case for the transpiration rate per unit of root length. The observed root length at
394 different soil depths (Figure 2) and total root length for two plots in the stony soil was much smaller than
395 in the silty soil (Figure 3). Therefore, transpiration per unit of root length in the stony soils (F1P2 & F1P3)

396 was almost 3 times higher than transpiration in the silty soil. For the same soil, transpiration per unit root
397 length of the irrigated treatment was slightly larger than in the rainfed plot.
398 The differences in sap flow per plant between water treatments and soil types were more pronounced in
399 2018 (Figure S9). The highest transpiration rate was observed in the irrigated plots (F1P3 & F2P3), followed
400 by the rainfed plot of the silty soil (F2P2) and it was lowest in the rainfed plot of the stony soil (F1P2).
401 These observations were in line with the differences in biomass and leaf area index between the
402 treatments (Figure S3b & S3d) and plant size (Figure S6b-c-d). In 2018, severe leaf rolling was observed in
403 the rainfed plot (F1P2) from the beginning of June until the end of the growing period in 2018 (Figure S3d).
404 Similar to 2017, transpiration per unit of root length was much higher in the stony plots as compared to
405 silty plots. Also, for the silty soil, transpiration per unit of root length of the irrigated plot (F2P3) was higher
406 than in the rainfed plot (F2P2).

407 Higher cumulative transpiration in the irrigated plots did not result in higher transpiration use efficiency
408 (TUE) in both soil types (Figure 10). For instance, TUE were 16.87 g mm^{-1} and 15.59 g mm^{-1} for F1P2 and
409 F2P2, respectively, while they were 15.47 and 14.79 g mm^{-1} for F1P3 and F2P3, respectively, in 2017 (Figure
410 10A). For the same soil, the rainfed plot showed slightly higher TUE than the irrigated plot. When
411 comparing the TUE of maize of the two soil types for the same water treatment, TUE at the stony soil was
412 almost the same in silty soil. The TUE was not much different among treatments and soil types in 2018.
413 Overall, TUE in 2017 was higher as compared to 2018 (Fig. 10b).

414 [Insert Figure 10 here]

415 **4. Discussions**

416 **4.1. Effects of soil types, water application, and climatic condition on root growth**

417 Our root observations showed that soil type affected root growth more than water treatment (Figure 2).
418 Root growth was strongly inhibited by the stony soil where much lower root length was observed than in

the silty soil, especially in the deeper soil layers. This was consistent with the findings reported in (Morandage et al., 2021) where a linear increase of stone content resulted in a linear decrease of rooting depth across all stone contents and developmental stages. Also, both simulations and observations indicated that rooting depth was increased due to the presence of cracks in the lower minirhizontron facility (Morandage et al., 2021) which could explain the high root length between 40 and 120 cm soil depths which was observed in the silty soil in both years.

In terms of the ratios of root length to shoot biomass, Ordóñez et al., (2020) has reported much larger figures of for instance 880 cm g^{-1} in different locations and under different N application rates in maize growing in the Midwest of US. Jorda et al., (2022) reported a wide range of ratios of root length to shoot biomass from 200 to 1000 cm g^{-1} around flowering time of maize depending on the wild type and root hair mutant genotypes growing on either loamy or sandy soils. More roots and higher ratios of root length to shoot biomass were found in the sand than in the loam in both wild type and root hair mutant genotypes (Jorda et al., 2022; Vetterlein et al., 2022). Cai et al., (2018) observed much larger ratios of root length to shoot biomass in drought stressed plots than in irrigated plot in both soil types in winter wheat which indicated the alternation of sink: source relationships to cope with water stress. This study emphasized that more assimilates are used to promote root growth and extract more water under drought stress. However, this was not the case for the stony soil in our work where the drought stress was more pronounced, especially in 2018. A drop of soil water potential (Figure S2b), thus effective soil water potential (Figure 6a) was substantial from 10th July 2018 toward the harvest in the rainfed plot in the silty soil (F2P2) which was consistent with the reduction of leaf water potential (Fig. 6b), leaf area (Figure S3c), total dry matter (Figure S3d), and crop height (Figure S6b) as compared the irrigated plot (F2P3). This indicates a mild water stress in 2018 in the rainfed plots on the silty soil. The larger ratios of root length to shoot biomass in this F2P2 plot in 2018 as compared to F2P3 could be explained by the change of source: sink relations where more assimilates were devoted to root growth, even at a later growth stage.

Moreover, the low stone content and soil cracks (Morandage et al., 2021) might favor root growth in the deeper soil layers which are close to the shallow soil water table in the rhizotrone facility with silty soil (Vanderborght et al., 2010). In conclusion, both soil texture and water conditions influenced the root growth, however, effects of the former on root length was more pronounced than the latter.

In the stony soil, which has a considerably smaller water holding capacity than the silty soil, root length was considerably smaller than in the silty soil. Nevertheless, water uptake per unit root length was much larger than in the fine soil. This also means that the hydraulic conductance per unit root length must have been much larger in the stony soil than in the fine soil. Cai et al., (2018) observed a similar effect for winter wheat but they found much smaller differences in the root length normalized root conductance. The higher root length normalized root conductance means that the anatomy of the root tissues must have been influenced by the soil texture and compensated the considerably smaller root length in the stony soil. Looking at the effect of water treatments in the silt soil, the non-irrigated plot had more roots than the irrigated one and both had more roots in the year with high VPD. But the soil-root conductance was higher in the irrigated plot than in the rainfed plot. This means that in the irrigated plot, the soil-root conductance per unit root length was higher than in the rainfed plot. This could either be due to wetter soil conditions and higher soil conductance or it could be due to a larger conductance of the root tissues. Especially in 2017 when the silty soil was wetter, the slightly larger soil-root conductance in the irrigated plot is most likely the result of larger root tissue conductance in the irrigated plot. Thus, how root architecture (here represented simply by the total root length) and root tissue conductivities 'respond' to drought stress might be opposite depending on the comparisons that are made. When the stony soil and silt soil are compared, the higher 'stress' due to lower water availability in the stony soil resulted in less roots with a higher root tissue conductance in the soil with more stress. When comparing the rainfed with the irrigated plot in the silty soil, the higher stress in the rainfed soil resulted in more roots with a lower

root tissue conductance in the treatment with more stress. This indicates that the response to water stress can be different depending on soil conditions or water treatments.

4.2. Effects of soil types, water application, and climatic condition on stomatal conductance, photosynthesis, transpiration, leaf water potential, and plant hydraulic conductance

4.2.1. Leaf water potential and stomatal conductance as affected by soil water conditions

In the previous work, Koehler et al., (2022) reported that maize stomata closed at lower negative leaf water potentials in sand than in loam growing under controlled environment. Cai et al., (2022b) investigated transpiration response of pot-grown maize in two contrasting soil textures (sand and loam) and exposed to two consecutive VPD levels (1.8 and 2.8 kPa). Transpiration rate decreased at less negative soil matric potential in sand than in loam at both VPD levels. In sand, high VPD generated a steeper drop in stomatal conductance with decreasing leaf water potential which indicated that the transpiration and stomatal responses depend on soil hydraulics. In our study, stomata closed earlier and at more negative soil and leaf water potentials in the stony soil than in the silty soil (see Fig. 4 & 7 and Figure S4 & S5). The lower soil water holding capacity of the stony soil compared to the silty soil resulted in lower soil water potential and smaller total plant hydraulic conductance which in turn led to earlier stomatal closure and to more negative soil water potential in the stony soil.

Stomatal control is an early and effective response to water stress to prevent the plant from water loss and dehydration. Maize is considered as an isohydric plant which closes its stomata to maintain leaf water potential above critical levels (Tardieu and Simonneau, 1998). Our results showed that minimum leaf water potential varied among treatments (-1.5 MPa for F1P3, F2P2, and F2P3 and up to -2 MPa for F1P2 in 2017, while in 2018 minimum values were -2 MPa for F2P3, F2P2, and F2P3 and -2.7 MPa for F1P2) (Fig. 5, Fig. 6, and Fig. 7). In conclusion, our results confirmed that the minimum ψ_{leaf} not only depended on

genotypic differences but also was influenced by soil types, soil hydraulic conductance, and atmospheric demand.

4.2.2. Hydraulic conductance components as affected by soil water conditions

Estimates of hydraulic components in soil-plant-atmosphere continuum are important not only to understand its underlying relationship to other crop characteristics (stomatal conductance, transpiration, and photosynthesis) but also to provide modeling parameters in process-based soil-root-shoot models (Nguyen et al., 2020; Sulis et al., 2019; Nguyen et al., 2022b). Measurement of the components of hydraulic conductance are challenging under field conditions because it requires the estimation of transpiration and root to leaf water potential gradients. To our knowledge, our results were unique with regard to the dynamics of K_{soil_plant} for field-grown maize on two soil types and under contrasting water, and climatic conditions. Our seasonal K_{soil_plant} ranged from 0.12 mm h^{-1} MPa^{-1} to 0.9 mm h^{-1} MPa^{-1} (Fig. 6 & Fig. 7; Fig. 8, and Figure S7). Root system hydraulic conductance ranged from 0.26 to 1.47 mm h^{-1} MPa^{-1} (Figure 9). Note that the unit of K_{soil_plant} as mm h^{-1} MPa^{-1} could be equivalent to the unit of 10^{-5} h^{-1} if one assumes 1MPa is approximately 10^5 mm in terms of pressure head. Cai et al., (2018) reported root hydraulic conductance in winter wheat from 0.05 to 0.5 mm h^{-1} MPa^{-1} in two similar soil types. Nguyen et al., (2020) also reported K_{soil_plant} in winter wheat from 0.0625 to 0.461 mm h^{-1} MPa^{-1}. Meunier et al., (2018) focused on estimating the root system hydraulic conductance of maize in a container experiment where the range of K_{soil_plant} was much larger from 0.37 to 36 mm h^{-1} MPa^{-1} for the plant density of 10 plant m^{-2}. Jorda et al., (2022) estimated root system hydraulic conductance of 0.5 to 1.5 10^{-3} d^{-1} which would be roughly between 2 to 6 mm h^{-1} MPa^{-1}. In our work, except the F2P2 in 2018, the stem hydraulic conductance was 10% to 60% higher than root system hydraulic conductance. Gallardo et al., (1996) reported that stem hydraulic conductance of wheat was lower than root system conductance at around 71 to 91 days after sowing (DAS), but they were similar at 102 DAS. In lupine, stem hydraulic conductance was two times higher than root system conductance regardless of measured days. The larger root length in wheat than lupine did not

necessarily result in higher root conductance in wheat. Together with this study, our study emphasizes the values of stem hydraulic conductance compared to the root hydraulic conductance in maintaining water potential gradient from shaded leaf or plant color to the sunlit leaf.

Our results showed clear differences in K_{soil_plant} among treatments where much lower K_{soil_plant} was observed in the F1P2 as compared to F2P2 (see Figure 8 for 2018; Figure 6 and 7 and Figure S7 for both years). This indicated the soil texture dependence for whole plant hydraulic conductance. Maize plants with the shorter root system (i.e. rainfed plot in the stony soil in 2018) (Fig. 3) had lower plant hydraulic conductance. Our results indicated that there was an impact of soil hydraulic conditions on K_{soil_plant} via the reduction of root system hydraulic conductance. Our analysis for three consecutive measurement days in 2018 (Fig 8) showed that in the silty soil, K_{soil_plant} decrease when soil water potentials are becoming more negative. For instance, in the silty soil in 2018 when the soil water potentials were considerably lower in the rainfed than in the irrigated plot (e.g. after 10^{th} July), K_{soil_plant} was lower in the rainfed than in the irrigated plot. In the stony soil, the K_{soil_plant} and leaf water potentials seems to decrease more considerably (compared to the silty soil) when the soil water potentials become more negative. In other words, K_{soil_plant} increased considerably when the soil water potentials in the stony soil increased. In our work, K_{soil_plant} increased slowly after irrigation mainly for the severe water stress plot (see F1P2 on 19 July in Fig 7d and 8c). This implied that added soil water by irrigation took some time for recovery the soil-root contact within the rhizophere.

4.2.3. Relationships of stomatal conductance, transpiration, photosynthesis with plant hydraulic variables

The transpiration rate and K_{soil_plant} (slope of linear regression lines in Fig. 8a and b) were very low in the rainfed plot under the stony soil (F1P2) which was associated with the large $\psi_{difference}$ (Fig. 8a & b) and the lower stomatal conductance as compared to other plots (Fig. 7c). The K_{soil_plant} slightly increased after irrigation (18 July - DOY 199 in Fig. 8b) corresponding with the smaller $\psi_{difference}$ (Fig. 8b) and an increase in

stomatal conductance (Fig. 7c). Seasonal K_{soil_plant} was low in the rainfed plot under stony soil (F1P2) with the larger $\psi_{difference}$ (Figure S7). In addition, our study showed that the midday stomatal conductance, photosynthesis, and transpiration were significantly correlated only with midday K_{soil_plant} in the rainfed plot on the stony soil (F1P2) in 2018 where high VPD and temperature occurred (Table S1, Figure S10, and S11). Maize plants had lower plant hydraulic conductance and more negative soil water potential in the rainfed plot in stony soil that and they exhibited earlier stomatal closure as compared to the same plot in the silty soil. This was in line with a study from Abdalla et al., (2022) which suggested that during soil drying, stomatal regulation of tomato is controlled by root and soil hydraulic conductance. Recent work from Müllers et al., (2022) on faba bean and maize suggested that differences in the stomatal sensitivity among plant species can be partly explained by the sensitivity of soil-plant hydraulic conductance to soil drying. The loss of conductance has immediate consequences for leaf water potential and the associated stomatal regulation. Cai et al., (2022b) also showed that the decrease in sunlit leaf stomatal conductance was well correlated with the drop in soil-plant hydraulic conductance, which was significantly affected by soil texture. This was confirmed in our work where the stony soil strongly impacted on root growth, modulated $K_{soil\_plant,}$ and consequently influenced the leaf stomatal conductance, photosynthesis, and transpiration.

4.3. Relative contribution of water control by leaves and roots on transpiration and transpiration use efficiency

Responses of crops via stomatal control to reduce water loss at leaf scale while maintaining leaf photosynthesis and water use efficiency were reported earlier (Nguyen et al., 2022a; Vitale et al., 2007). In addition to that, in the maize experiments in 2017 and 2018 leaf rolling was observed in both rainfed plots on the stony and the silty soil in the second week of June 2017 and from the beginning of June until the end of the growing period in 2018. This indicates another dehydration avoidance mechanism resulting from morphological adjustments which is an effective strategy to leaf senescence (Aparicio-Tejo and

Boyer, 1983; Richards et al., 2002). Stomatal closure resulted in more reduction of transpiration and assimilation in the rainfed plots than irrigated plots with the same soil type (Fig. 4, Figure S4 & S5, Fig. 5, and Figure S9a). There was reduction of shoot biomass (also stem size and leaf size adjustments) in F1P2 as compared to other plots. However, the TUE was not smaller in this plot than the remaining plots. These observations confirm that plant size adjustments through reduction of height, leaf width and length are efficient responses to reduce water loss at canopy scale in addition to stomatal control at the leaf level.

Relative contribution of leaf area to transpiration has been highlighted in wheat where reduction of tiller number resulted in significantly lower LAI, thus lower canopy transpiration (Cai et al., 2018; Trillo and Fernández, 2005; Nguyen et al., 2022a). However, root system conductance per unit of leaf area and per unit root mass were strongly reduced and eventually more than reduction of leaf area under water stress (Trillo and Fernández, 2005). In our work, expressing the transpiration per unit of root length on the one hand allowed to analyze the role of total root length to water uptake. However, on the other hand, the lower total root length did not necessarily result in a lower root water uptake and vice versa. For instance, the rainfed plot of the treatment F2P2 had the larger total root length which could postpone the effect of soil water limitations in drying soils due to greater ability to extract water from subsoils. Therefore, transpiration was very similar between F2P2 and F2P3. Despite of the much lower total root length in the stony soil, K_{soil_plant} in the irrigated plot (F1P3) was not much lower than in the same water treatment in the silty soil (F2P3, Fig. 6d, 7d, Fig. 8, and Figure S7). This could be explained by the fact that the K_{soil_plant} variability was not only depended on root architecture (here the root length and distribution) but also depended on the variability of root segment hydraulic properties which has also been illustrated and discussed in Zwieniecki et al. (2002), Frensch and Steudle (1989), Meunier et al. (2018), Couvreur et al. (2014), and Ahmed et al. (2018). Moreover, the contribution of shoot hydraulic conductance could be large in plants (Gallardo et al., 1996; Trillo and Fernández, 2005; Sunita et al., 2014) which also confirmed in our work. In our work, K_{soil_plant} comprised root and shoot conductance which are directly influenced by soil

584 hydraulics. Our estimates of K_{soil_plant} varied with transpiration and gradients of $\psi_{sunlitleaf}$ and ψ_{soil_effec}. Thus,
585 any change of soil hydraulic conductance will change the root to shoot water potential. Consequently, it
586 will affect the gradients between shoot and root rhizosphere (Carminati and Javaux, 2020). Thus, our study
587 is revealing the importance of both soil texture characteristics and root phenotypic traits (here root length)
588 in regulating plant transpiration (Cai et al., 2022a). Despite of lower root length in the stony irrigated plot,
589 transpiration rate was not much lower than in the silty irrigated plot in our work. This could be related to
590 another property of the root such as root segment conductance or other root traits (e.g. root hair). Further
591 investigation with extensive measurements of roots including axial and radial root conductance at field
592 scale will be required to better explain the observed results. Other traits like root hair density (Cai et al.,
593 2022a) or higher root length density (Vadez, 2014) could contribute to the soil to root water potential and
594 root-zone hydraulic conductance where dense root hairs are delaying soil water deficit in drying soils.
595 However, contrasting results have shown that root hairs did not have an effect on root water uptake (see
596 Jorda et al. 2022). The role of root hairs could not be analyzed in our work which was based on the root
597 data from minirhizotron images.

598 This study investigated soil-water-plant relations, more specifically the interactions of the root and shoot
599 growth processes and water fluxes under variations of soil water status and atmospheric demands. To the
600 best of our knowledge, the comprehensive data collected from soil to root, plant, and atmosphere under
601 field conditions in this work was unique. However, we acknowledged the lack of treatment replicates
602 which was due to the complex and expensive construction of the rhizotrone facilities. We also
603 acknowledged the small size of plots that did not allow the extensive destructive sampling (i.e. leaf area,
604 biomass, or determination of leaf water potential etc.). Each rhizotrone site originally contained the
605 irrigated, rainfed, and rain-out sheltered plots (Nguyen et al., 2022a; Cai et al., 2016). The overall aim of
606 the experiments was to investigate the root and shoot responses and gas fluxes (CO_2 and H_2O) of wheat
607 and maize to the variations of soil water and soil hydraulics. Note that the studies did not intend to

investigate the impacts of similar irrigation strategies on plant water status among seasons (i.e. in 2017 and 2018) because the irrigation practices were less common in the regions. The collapse of manual rain-out shelters due to strong wind after the 2016 growing season resulted in only two water treatments (rainfed and irrigated). Based on experiences from the previous seasons (wheat), we argued that such combinations of two water treatments and two soil types, to some extent, could still create a wide range of soil water conditions for the maize trial. For instance, the "rainfed" treatment at the stony soil in the upper rhizotrone (F1P2) could lead to severe water stress compared to other treatments, especially in the summertime when the atmospheric evaporative demand is high. In fact, mild water stress was observed at the F1P2 around mid -June in 2017. In 2018, the sites were slightly modified to induce more severe water stress (Nguyen et al., 2022a). One rainfed plot with the stony soil had late sowing while one rainfed plot with the silty soil had the higher sowing density (data not shown in the study). Unprecedented weather (extremely hot and dry) in 2018 resulted in severe drought stress at the rainfed plots with the stony soil. To compare the effects of soil types and water treatments on crop, we presented here only data from two plots (rainfed and irrigated) for two soil types. In spite of the experimental limitations, the relative differences among the treatments, soil types, and seasons as well as measured dates were clearly illustrated which ultimately supported the overall aim of our study.

The simultaneous measurements of atmospheric conditions, leaf water potential, and transpiration rates, coupled with measurements of root, stem and whole soil-plant hydraulic conductance, root architecture (root length), and soil water potential distribution illustrated the complex responses of the shoot and root growth and hydraulic conductance vulnerability to soil water availability. The different responses of crop processes to soil hydraulics and climatic conditions suggest further field investigations for other soil types, growing seasons, and water regimes. Future studies considering the effects of progressive soil drying or irrigation strategies on plant water status and crop growth at field conditions will be necessary. This is very relevant for those crop-growing regions that require irrigation. Our results show that the leaf water

potential threshold can vary within the same genotype depending on soil types, climatic conditions, and water management. Large variability of minimum leaf water potential has been reported for maize genotypes under greenhouse conditions (Welcker et al., 2011). Field studies are required concerning the stomatal functions, water relations, hydraulic vulnerability traits, and root: shoot responses, especially of different maize cultivars in responding to drought stress. This will suggest implications for selecting agronomic cultivars and traits under changing climates. Results from this study show that soil-crop models should focus not only on simulating stomatal regulations to capture the response to drought stress, but also require adequate representations of root and leaf growth and adjustments. The soil hydraulics strongly influenced soil water availability and crop growths. Regional applications of soil-crop models for simulating gas fluxes and crop growth processes and for estimating irrigation amounts must account for the environmental heterogeneity within the spatial simulation unit whereas the soil heterogeneity is the key variable.

5. Conclusion

We presented plant hydraulic characteristics and crop growth from root to shoot of maize under field-grown conditions with two soil types (silty and stony), each soil with two water regimes (irrigated and rainfed) for two growing seasons (2017, 2018). Our results confirmed that root length and ratios of root length to shoot biomass were modulated by soil types and water treatment but less by seasonal evaporative demand. Increase ratio of root length to shoot biomass was an important response of maize that allows plants to extract more water under drought stress that occurred rather in the silty soil but less in the stony soil due to the higher content of stony material.

Another conclusion is that stomatal regulation maintains leaf water potential at certain thresholds which depends on soil types, soil water availability, and seasonal atmospheric demand. The stomata conductance was smaller and decreased at more negative leaf water potentials in stony soil than in silty soil. The leaf water potentials are affected by the soil-plant hydraulic conductance. In addition to stomatal regulation,

leaf growth and plant size adjustments are important to regulate the transpiration and water use efficiency in the same year.

The lowest soil-plant hydraulic conductance was observed in the stony soil with severe drought stress as compared to silty soil while its variation depends also on the soil water variation (before and after irrigation). Root system and soil-plant hydraulic conductance depended strongly on soil hydraulic properties. The 'response' to stress can be completely opposite depending on conditions or treatments that lead to the differences in stress that are compared. Therefore, it cannot be the 'stress' alone that defines how a plant will react and adapt its root system. Modelling the impact of stress and the feedback between drought stress and plant development is likely controlled by other properties or parameters that change with changing soil water availability and atmospheric water demand then the plant stress level.

Acknowledgements

This work has partially been funded by Federal Ministry of Education and Research (BMBF) through European SUSCAP project – 031B0170B and COINS project - 01LL2204C and the Deutsche Forschungsgemeinschaft (DFG, German Research Foundation) under Germany's Excellence Strategy – EXC 2070 – 390732324. We acknowledge the support by the SFB/TR32 "Pattern in Soil–Vegetation–Atmosphere Systems: Monitoring, Modelling, and Data Assimilation" funded by the Deutsche Forschungsgemeinschaft (DFG). Thuy Nguyen and Thomas Gaiser also thank the DETECT – CRC 1502 research program which is funded by DFG. We thank Dr. Matthias Langensiepen for his supports and technical help in the TR32 project. We would like to thank all the student assistants and technicians for their considerable efforts to collect the data in the field and the laboratories.

Reference

Abdalla, M., M.A. Ahmed, G. Cai, F. Wankmüller, N. Schwartz, et al. 2022. Stomatal closure during water deficit is controlled by below-ground hydraulics. Ann. Bot. 129(2): 161–170. doi: 10.1093/aob/mcab141.

Abdalla, M., A. Carminati, G. Cai, M. Javaux, and M.A. Ahmed. 2021. Stomatal closure of tomato under drought is driven by an increase in soil-root hydraulic resistance. Plant. Cell Environ. 44(2): 425–431. doi: 10.1111/pce.13939.

Ahmed, M.A., M. Zarebanadkouki, F. Meunier, M. Javaux, A. Kaestner, et al. 2018. Root type matters: Measurement of water uptake by seminal, crown, and lateral roots in maize. J. Exp. Bot. 69(5): 1199–1206. doi: 10.1093/jxb/erx439.

Allen, R.G., Pereira, L.S., Raes, D., Smith, M., 1998. FAO Irrigation and Drainage Paper – Crop Evapotranspiration. FAO, Italy.

Aparicio-Tejo, P., and J.S. Boyer. 1983. Significance of Accelerated Leaf Senescence at Low Water Potentials for Water Loss and Grain Yield in Maize1. Crop Sci. 23(6): cropsci1983.0011183X002300060040x. doi: https://doi.org/10.2135/cropsci1983.0011183X002300060040x.

Bauer, F.M., L. Lärm, S. Morandage, G. Lobet, J. Vanderborght, et al. 2021. Combining deep learning and automated feature extraction to analyze minirhizotron images: development and validation of a new pipeline. bioRxiv (1): 2021.12.01.470811. https://www.biorxiv.org/content/10.1101/2021.12.01.470811v1%0Ahttps://www.biorxiv.org/content/10.1101/2021.12.01.470811v1.abstract.

Bornemann*, L., M. Herbst, G. Welp, H. Vereecken, and W. Amelung. 2011. Rock Fragments Control Size and Saturation of Organic Carbon Pools in Agricultural Topsoil. Soil Sci. Soc. Am. J. 75(5): 1898. doi: 10.2136/sssaj2010.0454.

Bourbia, I., C. Pritzkow, and T.J. Brodribb. 2021. Herb and conifer roots show similar high sensitivity to water deficit. Plant Physiol. 186(4): 1908–1918. doi: 10.1093/plphys/kiab207.

Cai, G., M.A. Ahmed, M. Abdalla, and A. Carminati. 2022a. Root hydraulic phenotypes impacting water uptake in drying soils. Plant Cell Environ. 45(3): 650–663. doi: 10.1111/pce.14259.

Cai, G., M. König, A. Carminati, M. Abdalla, M. Javaux, et al. 2022b. Transpiration response to soil drying and vapor pressure deficit is soil texture specific. Plant Soil (0123456789). doi: 10.1007/s11104-022-05818-2.

Cai, G., J. Vanderborght, V. Couvreur, C.M. Mboh, and H. Vereecken. 2017a. Parameterization of Root Water Uptake Models Considering Dynamic Root Distributions and Water Uptake Compensation. Vadose Zo. J. 0(0): 0. doi: 10.2136/vzj2016.12.0125.

Cai, G., J. Vanderborght, A. Klotzsche, J. van der Kruk, J. Neumann, et al. 2016. Construction of Minirhizotron Facilities for Investigating Root ZoneProcesses. Vadose Zo. J. 15(9): 0. doi: 10.2136/vzj2016.05.0043.

Cai, G., J. Vanderborght, M. Langensiepen, A. Schnepf, H. Hüging, et al. 2018. Root growth, water uptake, and sap flow of winter wheat in response to different soil water conditions. Hydrol. Earth Syst. Sci. 22(4): 2449–2470. doi: 10.5194/hess-22-2449-2018.

Cai, Q., Y. Zhang, Z. Sun, J. Zheng, W. Bai, et al. 2017b. Morphological plasticity of root growth under mild water stress increases water use efficiency without reducing yield in maize. Biogeosciences 14(16): 3851–3858. doi: 10.5194/bg-14-3851-2017.

Carminati, A., and M. Javaux. 2020. Soil Rather Than Xylem Vulnerability Controls Stomatal Response to Drought. Trends Plant Sci. 25(9): 868–880. doi: 10.1016/j.tplants.2020.04.003.

720 Carminati, A., M. Zarebanadkouki, E. Kroener, M.A. Ahmed, and M. Holz. 2016. Biophysical rhizosphere
721 processes affecting root water uptake. Ann. Bot. 118(4): 561–571. doi: 10.1093/aob/mcw113.

722 Choudhary, S., and T.R. Sinclair. 2014. Hydraulic conductance differences among sorghum genotypes to
723 explain variation in restricted transpiration rates. Funct. Plant Biol. 41(3): 270–275. doi:
724 10.1071/FP13246.

725 Cochard, H. 2002. Xylem embolism and drought-induced stomatal closure in maize. Planta 215(3): 466–
726 471. doi: 10.1007/s00425-002-0766-9.

727 Comas, L.H., S.R. Becker, V.M. V. Cruz, P.F. Byrne, and D.A. Dierig. 2013. Root traits contributing to plant
728 productivity under drought. Front. Plant Sci. 4(NOV): 1–16. doi: 10.3389/fpls.2013.00442.

729 Coupel-Ledru, A., É. Lebon, A. Christophe, A. Doligez, L. Cabrera-Bosquet, et al. 2014. Genetic variation in
730 a grapevine progeny (Vitis vinifera L. cvs GrenachexSyrah) reveals inconsistencies between
731 maintenance of daytime leaf water potential and response of transpiration rate under drought. J.
732 Exp. Bot. 65(21): 6205–6218. doi: 10.1093/jxb/eru228.

733 Couvreur, V., J. Vanderborght, X. Draye, and M. Javaux. 2014. Dynamic aspects of soil water availability for
734 isohydric plants: Focus on root hydraulic resistances. water Resour. Res. 50: 8891–8906. doi:
735 10.1002/2014WR015608.Received.

736 Couvreur, V., J. Vanderborght, and M. Javaux. 2012. A simple three-dimensional macroscopic root water
737 uptake model based on the hydraulic architecture approach. Hydrol. Earth Syst. Sci. 16: 2957–2971.
738 doi: 10.5194/hess-16-2957-2012.

739 Daryanto, S., L. Wang, and P. Jacinthe. 2016. Global Synthesis of Drought Effects on Maize and Wheat
740 Production. PLoS One 11(5): 1–15. doi: 10.1371/journal.pone.0156362.

741 Draye, X., Y. Kim, G. Lobet, and M. Javaux. 2010. Model-assisted integration of physiological and
742 environmental constraints affecting the dynamic and spatial patterns of root water uptake from
743 soils. J. Exp. Bot. 61(8): 2145–2155. doi: 10.1093/jxb/erq077.

744 Domec, J., and D.M. Johnson. 2012. Does homeostasis or disturbance of homeostasis in minimum leaf
745 water potential explain the isohydric versus anisohydric behavior of Vitis vinifera L . cultivars ? Tree
746 32: 245–248. doi: 10.1093/treephys/tps013.

747 Domec, J., and M.L. Pruyn. 2008. Bole girdling affects metabolic properties and root , trunk and branch
748 hydraulics of young ponderosa pine trees. Tree Physiol. (28): 1493–1504.

749 Dynamax. 2007. Dynagage Sap Flow Sensor User Manual. 1–107. Last access on March 5th 2015.

750 Effendi, R., S.B. Priyanto, M. Aqil, and M. Azrai. 2019. Drought adaptation level of maize genotypes based
751 on leaf rolling, temperature, relative moisture content, and grain yield parameters. IOP Conf. Ser.
752 Earth Environ. Sci. 270(1). doi: 10.1088/1755-1315/270/1/012016.

753 Fang, J., and Y. Su. 2019. Effects of Soils and Irrigation Volume on Maize Yield, Irrigation Water Productivity,
754 and Nitrogen Uptake. Sci. Rep. 9(1): 1–11. doi: 10.1038/s41598-019-41447-z.

755 Frensch, J., and E. Steudle. 1989. Axial and Radial Hydraulic Resistance to Roots of Maize (Zea mays L.).
756 Plant Physiol. 91: 719–726.

757 Gallardo, M., J. Eastham, P.J. Gregory, and N.C. Turner. 1996. A comparison of plant hydraulic
758 conductances in wheat and lupins. J. Exp. Bot. 47(295): 233–239. doi: 10.1093/jxb/47.2.233.

759 Hochberg, U., F.E. Rockwell, N.M. Holbrook, and H. Cochard. 2018. Iso/Anisohydry: A Plant–Environment
760 Interaction Rather Than a Simple Hydraulic Trait. Trends Plant Sci. 23(2): 112–120. doi:
761 10.1016/j.tplants.2017.11.002.

762 Hopmans, J.W., and K.L. Bristow. 2002. Current Capabilities and Future Needs of Root Water and
763 Nutrient Uptake Modeling. In: Sparks, D.L.B.T.-A. in A., editor, Advances in Agronomy. Academic
764 Press. p. 103–183

765 Hubbard, R.M., M.G. Ryan, V. Stiller, and J.S. Sperry. 2001. Stomatal conductance and photosynthesis vary
766 linearly with plant hydraulic conductance in ponderosa pine. Plant, Cell Environ. 24(1): 113–121. doi:
767 10.1046/j.1365-3040.2001.00660.x.

768 IPCC. 2022. Impacts, Adaptation, and Vulnerability. Working Group II Contribution to the IPCC Sixth
769 Assessment Report of the Intergovernmental Panel on Climate Change.

770 Jorda, H., M.A. Ahmed, M. Javaux, A. Carminati, P. Duddek, et al. 2022. Field scale plant water relation of
771 maize (Zea mays) under drought – impact of root hairs and soil texture. Plant Soil 478(1–2): 59–84.
772 doi: 10.1007/s11104-022-05685-x.

773 Klein, T. 2014. The variability of stomatal sensitivity to leaf water potential across tree species indicates a
774 continuum between isohydric and anisohydric behaviours. Funct. Ecol.: 1313–1320. doi:
775 10.1111/1365-2435.12289.

776 Koehler, T., D.S. Moser, Á. Botezatu, T. Murugesan, S. Kaliamoorthy, et al. 2022. Going underground: soil
777 hydraulic properties impacting maize responsiveness to water deficit. Plant Soil 478(1–2): 43–58. doi:
778 10.1007/s11104-022-05656-2.

779 Lärm, L., F.M. Bauer, N. Hermes, J. van der Kruk, H. Vereecken, et al. 2023. Multi-year belowground data
780 of minirhizotron facilities in Selhausen. Sci. Data 10(1): 1–15. doi: 10.1038/s41597-023-02570-9.

781 Li, X., T.R. Sinclair, and L. Bagherzadi. 2016. Hydraulic Conductivity Changes in Soybean Plant-Soil System
782 with Decreasing Soil Volumetric Water Content. J. Crop Improv. 30(6): 713–723. doi:
783 10.1080/15427528.2016.1231729.

784 Li, Y., J.S. Sperry, and M. Shao. 2009. Hydraulic conductance and vulnerability to cavitation in corn (Zea
785 mays L.) hybrids of differing drought resistance. Environ. Exp. Bot. 66(2): 341–346. doi:
786 10.1016/j.envexpbot.2009.02.001.

787 Marin, M., D.S. Feeney, L.K. Brown, M. Naveed, S. Ruiz, et al. 2021. Significance of root hairs for plant
788 performance under contrasting field conditions and water deficit. Ann. Bot. 128(1): 1–16. doi:
789 10.1093/aob/mcaa181.

790 Meunier, F., A. Heymans, X. Draye, V. Couvreur, M. Javaux, et al. 2020. MARSHAL, a novel tool for virtual
791 phenotyping of maize root system hydraulic architectures. In Silico Plants 2(1): 1–15. doi:
792 10.1093/insilicoplants/diz012.

793 Meunier, F., M. Zarebanadkouki, M.A. Ahmed, A. Carminati, V. Couvreur, et al. 2018. Hydraulic
794 conductivity of soil-grown lupine and maize unbranched roots and maize root-shoot junctions. J.
795 Plant Physiol. 227(February): 31–44. doi: 10.1016/j.jplph.2017.12.019.

796 Morandage, S., J. Vanderborght, M. Zörner, G. Cai, D. Leitner, et al. 2021. Root architecture development
797 in stony soils. Vadose Zo. J. (April): 1–17. doi: 10.1002/vzj2.20133.

798 Müllers, Y., J.A. Postma, H. Poorter, and D. van Dusschoten. 2022. Stomatal conductance tracks soil-to-leaf

799 hydraulic conductance in faba bean and maize during soil drying. Plant Physiol. doi:
800 10.1093/plphys/kiac422.

801 Nguyen, T.H., M. Langensiepen, T. Gaiser, H. Webber, H. Ahrends, et al. 2022a. Responses of winter wheat
802 and maize to varying soil moisture: From leaf to canopy. Agric. For. Meteorol. 314(December 2021):
803 108803. doi: 10.1016/j.agrformet.2021.108803.

804 Nguyen, T.H., M. Langensiepen, H. Hueging, T. Gaiser, S.J. Seidel, et al. 2022b. Expansion and evaluation
805 of two coupled root–shoot models in simulating CO2 and H2O fluxes and growth of maize. Vadose
806 Zo. J. 21(3): 1–31. doi: 10.1002/vzj2.20181.

807 Nguyen, T.H., M. Langensiepen, J. Vanderborght, H. Hüging, C.M. Mboh, et al. 2020. Comparison of root
808 water uptake models in simulating CO2 and H2O fluxes and growth of wheat. Hydrol. Earth Syst. Sci.
809 (24): 4943–4969. doi: 10.5194/hess-24-4943-2020.

810 Nguyen, T.H, G. Lopez, S.J. Seidel, L. Lärm, F.M. Bauer, et al. 2024b. Multi-year aboveground data of
811 minirhizotron facilities in Selhausen. Sci. Data 11(1): 1–11. doi.org/10.1038/s41597-024-03535-2

812 Ordóñez, R.A., S. V. Archontoulis, R. Martinez-Feria, J.L. Hatfield, E.E. Wright, et al. 2020. Root to shoot
813 and carbon to nitrogen ratios of maize and soybean crops in the US Midwest. Eur. J. Agron. 120(June):
814 126130. doi: 10.1016/j.eja.2020.126130.

815 Passioura, J.B., 2006. The perils of pot experiments. Funct. Plant Biol. 33 (12), 1075–1079.
816 https://doi.org/10.1071/FP06223.

817 Ranawana SRWMCJK, Siddique KHM, Palta JA et al (2021) Stomata coordinate with plant hydraulics to
818 regulate transpiration response to vapour pressure defcit in wheat. Functional Plant Biol 48:839–850.
819 https://doi.org/10.1071/FP20392

820 Richards, R.A., G.J. Rebetzke, A.G. Condon, and A.F. van Herwaarden. 2002. Breeding Opportunities for
821 Increasing the Efficiency of Water Use and Crop Yield in Temperate Cereals. Crop Sci. 42(1): 111–
822 121. doi: 10.2135/cropsci2002.1110.

823 Rodriguez-Dominguez, C.M., and T.J. Brodribb. 2019. Declining root water transport drives stomatal
824 closure in olive under. New Phytol. 225: 126–134.

825 Sinclair, T.R., and M.M. Ludlow. 1986. Influence of soil water supply on the plant water balance of four
826 tropical grain legumes. Aust. J. Plant Physiol. 13: 329–341.

827 Scharwies, J.D., and J.R. Dinneny. 2019. Water transport, perception, and response in plants. J. Plant Res.
828 132(3): 311–324. doi: 10.1007/s10265-019-01089-8.

829 Schultz, H.R. 2003. Differences in hydraulic architecture account for near-isohydric and anisohydric
830 behaviour of two field-grown Vitis vinifera L. cultivars during drought. Plant, Cell Environ. 26(8):
831 1393–1405. doi: 10.1046/j.1365-3040.2003.01064.x.

832 Stadler, A., S. Rudolph, M. Kupisch, M. Langensiepen, J. van der Kruk, et al. 2015. Quantifying the effects
833 of soil variability on crop growth using apparent soil electrical conductivity measurements. Eur. J.
834 Agron. 64: 8–20. doi: 10.1016/j.eja.2014.12.004.

835 Sulis, M., V. Couvreur, J. Keune, G. Cai, I. Trebs, et al. 2019. Incorporating a root water uptake model based
836 on the hydraulic architecture approach in terrestrial systems simulations. Agric. For. Meteorol. 269–
837 270: 28–45. doi: https://doi.org/10.1016/j.agrformet.2019.01.034.

838 Sunita, C., T.R. Sinclair, C.D. Messina, and M. Cooper. 2014. Hydraulic conductance of maize hybrids

differing in transpiration response to vapor pressure deficit. Crop Sci. 54(3): 1147–1152. doi: 10.2135/cropsci2013.05.0303.

Tardieu, F., X. Draye, and M. Javaux. 2017. Root Water Uptake and Ideotypes of the Root System: Whole-Plant Controls Matter. Vadose Zo. J. 16(9): 0. doi: 10.2136/vzj2017.05.0107.

Tardieu, F., and T. Simonneau. 1998. Variability among species of stomatal control under fluctuating soil water status and evaporative demand: modelling isohydric and anisohydric behaviours. J. Exp. Bot. 49(March): 419–432. doi: 10.1093/jxb/49.Special_Issue.419.

Tardieu, F. 2016. Too many partners in root – shoot signals . Does hydraulics qualify as the only signal that feeds back over time for reliable stomatal. New Phytol. 212: 802–804.

Trillo, N., and R.J. Fernández. 2005. Wheat plant hydraulic properties under prolonged experimental drought: Stronger decline in root-system conductance than in leaf area. Plant Soil 277(1–2): 277–284. doi: 10.1007/s11104-005-7493-5.

Tsuda, M., and M.T. Tyree. 1997. Whole-plant hydraulic resistance and vulnerability segmentation in Acer saccharinum. Tree Physiol. (17): 351–357.

Turner, N.C., E.D. Schulze, and T. Gollan. 1984. The responses of stomata and leaf gas exchange to vapour pressure deficits and soil water content - I. Species comparisons at high soil water contents. Oecologia 63(3): 338–342. doi: 10.1007/BF00390662.

Tyree, M.T., E.L. Fiscus, S.D. Wullschleger, and M.A. Dixon. 1986. Detection of Xylem Cavitation in Corn under Field Conditions. Plant Physiol. 82(2): 597–599. doi: 10.1104/pp.82.2.597.

Vadez, V. 2014. Root hydraulics : The forgotten side of roots in drought adaptation. F. Crop. Res. 165: 15–24.

Vadez, V., S. Choudhary, J. Kholová, C.T. Hash, R. Srivastava, et al. 2021. Transpiration efficiency: Insights from comparisons of C4cereal species. J. Exp. Bot. 72(14): 5221–5234. doi: 10.1093/jxb/erab251.

Vanderborght, J., V. Couvreur, F. Meunier, A. Schnepf, H. Vereecken, et al. 2021. From hydraulic root architecture models to macroscopic representations of root hydraulics in soil water flow and land surface models. Hydrol. Earth Syst. Sci. 25(9): 4835–4860. doi: 10.5194/hess-25-4835-2021.

Vanderborght, J., A. Graf, C. Steenpass, B. Scharnagl, N. Prolingheuer, et al. 2010. Within-Field Variability of Bare Soil Evapora Θ on Derived from Eddy Covariance Measurements. Vadose Zo. J. 9: 943–954. doi: 10.2136/vzj2009.0159.

Vereecken, H., A. Schnepf, J.W. Hopmans, M. Javaux, D. Or, et al. 2016. Modeling Soil Processes: Review, Key Challenges, and New Perspectives. Vadose Zo. J. 15(5): vzj2015.09.0131. doi: 10.2136/vzj2015.09.0131.

Vetterlein, D., M. Phalempin, E. Lippold, S. Schlüter, S. Schreiter, et al. 2022. Root hairs matter at field scale for maize shoot growth and nutrient uptake, but root trait plasticity is primarily triggered by texture and drought. Plant Soil 478(1–2): 119–141. doi: 10.1007/s11104-022-05434-0.

Vitale, L., P. Di Tommasi, C. Arena, A. Fierro, A. Virzo De Santo, et al. 2007. Effects of water stress on gas exchange of field grown Zea mays L. in Southern Italy: An analysis at canopy and leaf level. Acta Physiol. Plant. 29(4): 317–326. doi: 10.1007/s11738-007-0041-6.

Wang, N., J. Gao, and S. Zhang. 2017. Overcompensation or limitation to photosynthesis and root hydraulic conductance altered by rehydration in seedlings of sorghum and maize. Crop J. 5(4): 337–344. doi:

10.1016/j.cj.2017.01.005.

Weihermüller, L., Huisman, J. A., Lambot, S., Herbst, M., & Vereecken, H. (2007). Mapping the spatial variation of soil water content at the field scale with different ground penetrating radar techniques. Journal of Hydrology, 340, 205–216. https://doi.org/10.1016/j.jhydrol.2007. 04.013

Welcker, C., W. Sadok, G. Dignat, M. Renault, S. Salvi, et al. 2011. A common genetic determinism for sensitivities to soil water deficit and evaporative demand: Meta-analysis of quantitative trait loci and introgression lines of maize. Plant Physiol. 157(2): 718–729. doi: 10.1104/pp.111.176479.

Zhuang, J., Y. Jin, and T. Miyazaki. 2001. ESTIMATING WATER RETENTION CHARACTERISTIC FROM SOIL PARTICLE-SIZE DISTRIBUTION USING A NON-SIMILAR MEDIA CONCEPT. Soil Sci. 166(5). https://journals.lww.com/soilsci/Fulltext/2001/05000/ESTIMATING_WATER_RETENTION_CHARACTERISTIC_FROM.2.aspx.

Zwieniecki, M.A., P.J. Melcher, C.K. Boyce, L. Sack, and N.M. Holbrook. 2002. Hydraulic architecture of leaf venation in Laurus nobilis L. Plant, Cell Environ. 25(11): 1445–1450. doi: 10.1046/j.1365-3040.2002.00922.x.

Author contribution

Huu Thuy Nguyen, Thomas Gaiser, Jan Vanderborght, and Frank Ewert: Conceptualization; Huu Thuy Nguyen, and Hubert Hüging: Data curation and data quality check (aboveground measurements); Lena Lärm, Felix Bauer, Anja Klotzsche, Jan Vanderborght, and Andrea Schnepf: data curation and data quality check (belowground measurements); Huu Thuy Nguyen: Formal data analysis and visualization; Thomas Gaiser, Jan Vanderborght, Andrea Schnepf, and Frank Ewert: Funding acquisition & Project administration; Huu Thuy Nguyen: writing – original draft; all authors: review, editing, and finalizing the manuscript.

Competing interests

This manuscript has not been published and is not under consideration for publication in any other journal. All authors agreed and approved the manuscript and its submission to this journal. We declare there is no conflict of interest.

Code/Data availability

The meteorological data were collected from a weather station in Selhausen (Germany) which belongs to the TERENO network of terrestrial observatories. Weather data are freely available from the TERENO data portal (https://www.tereno.net/ddp/dispatch?searchparams=freetext-Selhausen, last access: October 2020) (TERENO, 2020). The data which were obtained from the minirhizotron facilities (under- and aboveground) are publicly available in Lärm et al., (2023) and in Nguyen et al., (2024), respectively.

List of Tables

Table 1. Crop phenology and management information for different treatments in 2017 and 2018.

	2017				2018			
Soil types	Stony (F1)	Stony (F1)	Silty (F2)	Silty (F2)	Stony (F1)	Stony (F1)	Silty (F2)	Silty (F2)
Water treatments	Rainfed (P2)	Irrigated (P3)	Rainfed (P2)	Irrigated (P3)	Rainfed (P2)	Irrigated (P3)	Rainfed (P2)	Irrigated (P3)
Plot names	F1P2	F1P3	F2P2	F2P3	F1P2	F1P3	F2P2	F2P3
Growing season (days)[¥]	136	136	136	136	107	107	107	107
Cumulative rainfall (mm)[*]	248.7	248.7	248.7	248.7	91.3	91.3	91.3	91.3
Irrigation (mm)	0	130	0	130	66	257.6	0	257.6
Fertilizer application (mm/dd) (per hectare)	05/09:100 kg N + 40kg P_2O_5 07/06: 80 kg N + 40 kg K_2O				05/22: 100 kg N 05/30: 40 kg P_2O_5 + 40 kg K_2O 06/27: 80 kg N			
Sowing date (mm/dd)	05/04				05/08			
Emergence date	05/09				05/13			
Tasseling date	07/09				07/09			
Silking date	07/14				07/11			
Harvest date	09/12				08/22			

Notes: [¥] from sowing to harvest; [*] for rainfall for whole growing season;

List of Figures

Figure 1: Daily maximum air temperature (Tmax) (°C), daily maximum air vapor pressure deficit (VPD) (kPa) in the two growing seasons (a) 2017 and (b) 2018 and cumulative (sum) of rainfall and irrigation from the rainfed (P2) and irrigated (P3) plots of the stony soil (F1) and silty soil (F2) in the two growing seasons (c) 2017 and (d) 2018. The black dashed vertical lines (a) and (b) indicate silking time. Grey vertical lines in (a) and (b) indicate the measured days for leaf gas exchange and leaf water potential. Two lines for 2017F2P2 and 2017F2P3 were overlapped by the lines from 2017F1P2 and 2017F1P3, respectively

Figure 2: Observed root length from minirhizotubes (cm cm^{-2}) from 10, 20, 40, 60, 80, and 120 cm soil depth from the rainfed (P2) and irrigated (P3) plots of the stony soil (F1) and silty soil (F2) in the two growing seasons in 2017 (a - 8 June, b - at silking on 13 July, c - at harvest on 12 September) and in 2018 (d - 7 June, e - at one week after silking - 18 July, f - one week before harvest - 16 August).

926 Figure 3: Observed root length from minirhizotubes (m m^{-2}) and ratio of root length per shoot dry matter
927 (m kg^{-1}) from the rainfed (P2) and irrigated (P3) plots of the stony soil (F1) and silty soil (F2) in the two
928 growing seasons (DOY 159, 194, and 255, left panel) in 2017 and in 2018 (DOY 158, 199, and 228, right
929 panel) where on 8 June (DOY 159) at silking on 13 July (DOY194) 2017; and at harvest on 12 September
930 (DOY 255) in 2017; 7 June (DOY 158), one week after silking on 18 July (DOY 199); and one week before
931 harvest on 16 August (DOY 228) in 2018 (see also Figure 2).

932 Figure 4. Diurnal course of (a) photosynthetically active radiation (PAR) and vapor pressure deficit (VPD),
933 (b –e) leaf net photosynthesis (An), (f –i) leaf stomatal conductance (Gs), (j –m) leaf transpiration (E), and
934 (n –q) leaf water potential (LWP) on 18 July in maize in 2018 before irrigation at the rainfed (P2) and
935 irrigated (P3) plots of the stony soil (F1) and silty soil (F2). Measurement was carried out from shaded leaf
936 (plus symbol with line) and two sunlit leaves (solid dot - lines and solid square - lines). Crop was irrigated
937 at 1 PM, 1 PM, 4 PM for F1P3, F2P3, and F1P2, respectively (22.75 mm for each plot) (Supp. 2). Black
938 arrows indicate time of irrigation.

939 Figure 5: Seasonal stomatal conductance to water vapor (Gs) versus leaf water potential (ψ_{leaf}) in 2017 (top
940 panel) and in 2018 (bottom panel) at the rainfed (P2) and irrigated (P3) plots of the stony soil (F1) and silty
941 soil (F2). Vertically continuous and dashed lines indicated ψ_{leaf} at -1.5 and -2 MPa, respectively.
942 Measurement was carried out from shaded leaf (plus symbol) and two sunlit leaves (solid dots)

943 Figure 6: Dynamic of around midday (MD) of (a) the effective soil water potential ($\psi_{soil\_effec,\ MD}$) (b) sunlit
944 leaf water potential ($\psi_{sunlitleaf\ MD}$), (c) stomatal conductance (Gs MD) and (d) whole soil-plant hydraulic
945 conductance ($K_{soil\_plant\ MD}$) in the growing season 2017 from the rainfed (P2) and irrigated (P3) plots of the
946 stony soil (F1) and silty soil (F2). Error bars indicate the standard deviation of the different values taken
947 around midday (11 AM, 12AM, 1PM, and 2 PM) of different sunlit leaves. Whole soil-plant hydraulic
948 conductance was shown from 17 July when sap flow was measured. The black arrows indicates the
949 irrigation events for the irrigated treatments F1P3 and F2P3 in the showing period.

950 Figure 7: Dynamic of around midday (MD) of (a) the effective soil water potential ($\psi_{soil\_effec\ MD}$) (b) sunlit
951 leaf water potential ($\psi_{sunlitleaf\ MD}$), (c) stomatal conductance (Gs MD) and (d) whole soil-plant hydraulic
952 conductance ($K_{soil\_plant\ MD}$) in the growing season 2018 from the rainfed (P2) and irrigated (P3) plots of the
953 stony soil (F1) and silty soil (F2). Error bars indicate the standard deviation of the different values taken
954 around midday (11 AM, 12AM, 1PM, and 2 PM) Leaf water potential and stomatal conductance were 2
955 sunlit leaves and one shaded leaf at each measured hour. Whole soil-plant hydraulic conductance was
956 shown from 3 July when sap flow was measured. The black arrows indicates the irrigation events for the

957 irrigated treatments F1P3 and F2P3 while the orange arrow indicates the irrigation application for the
958 rainfed plot at the stony soil (F1P2).

959 Figure 8: Relationship of sap flow and difference of effective soil water potential and sunlit leaf water
960 potential ($\psi_{difference}$) from the rainfed (P2) and irrigated (P3) plots of the stony soil (F1) and silty soil (F2) on
961 three consecutive measurement days from predawn in 2018 (a) 17 July - DOY 198, (b) 18 July - DOY 199
962 and (c) 19 July - DOY 200. Crop was irrigated on 18 July (DOY 199) at 1 PM, 1 PM, and 4 PM for F1P3, F2P3,
963 and F1P2, respectively (22.75 mm for each plot). The unit of slope in the linear regression (or soil-plant
964 hydraulic conductance) is mm h^{-1} MPa^{-1}. Regression was based on the DEMING approach. The asterisk
965 which are next to the slopes indicate a significant correlation between two variables according to Pearson
966 method (ns: non-significant; * $p < 0.05$; ** $p < 0.01$; *** $p < 0.001$)

967 Figure 9: Comparison of different midday hydraulic components (mm h^{-1} MPa^{-1}): soil-plant (grey bars), soil-
968 root (yellow bars), and stem (blue bars) from the rainfed (P2) and irrigated (P3) plots of the stony soil (F1)
969 and silty soil (F2) in the two growing seasons (a) in 2017 and (b) in 2018. The error bars indicate the
970 standard deviation from measurements around midday (11 AM, 12AM, 1PM, and 2 PM) in different
971 measured days (in 2017 with n = 4 x 9 days, Supplementary material 10, 11, and Fig. 6 and in 2018 with n
972 = 4 x 10 days, Supplementary material 10, 12, and Fig. 7).

973 Figure 10: Relationship of aboveground dry matter and cumulative sap flow from the rainfed (P2) and
974 irrigated (P3) plots of the stony soil (F1) and silty soil (F2) in the two growing seasons (a) 2017 and (b) 2018.
975 The unit of slope linear relationship is g mm^{-1}. The less number of data points in (b) in 2018 from the F2P2
976 and F2P3 plots were due to the missing values of measured sap flow because of sensor disconnection. For
977 aboveground dry matter, each point represents the average of two sampling replicates, except the harvest
978 with 5 sampling replicates.

979

980

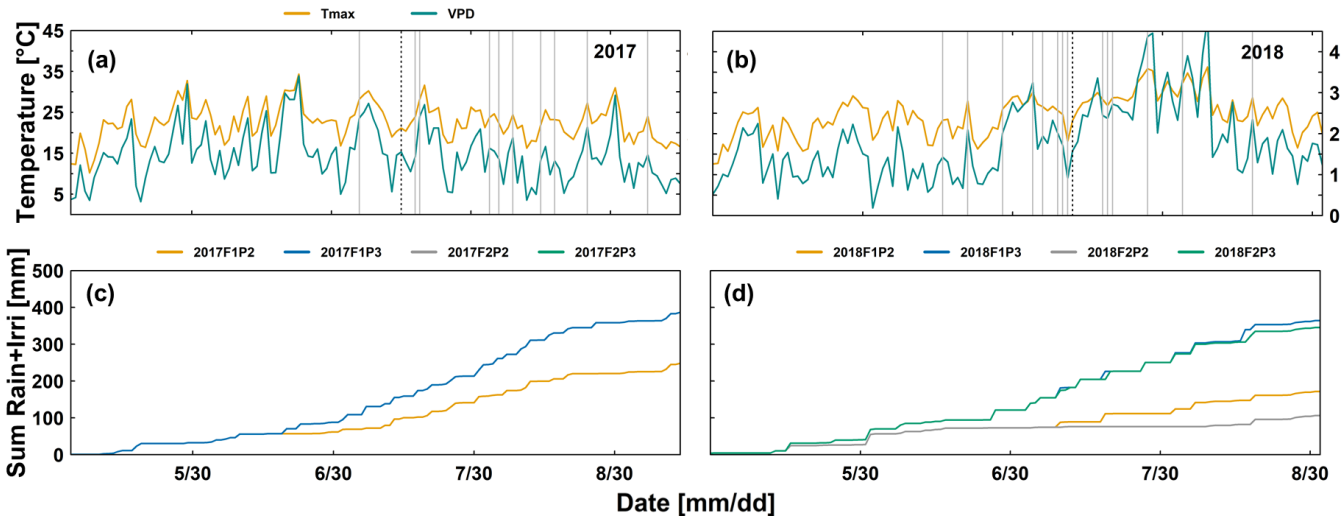
Tmax
VPD
(a)
2017
(b)
2018
Temperature [°C]
45
35
25
15
5
4
3
2
1
0
2017F1P2
2017F1P3
2017F2P2
2017F2P3
2018F1P2
2018F1P3
2018F2P2
2018F2P3
(c)
(d)
Sum Rain+Irri [mm]
500
400
300
200
100
0
5/30
6/30
7/30
8/30
Date [mm/dd]

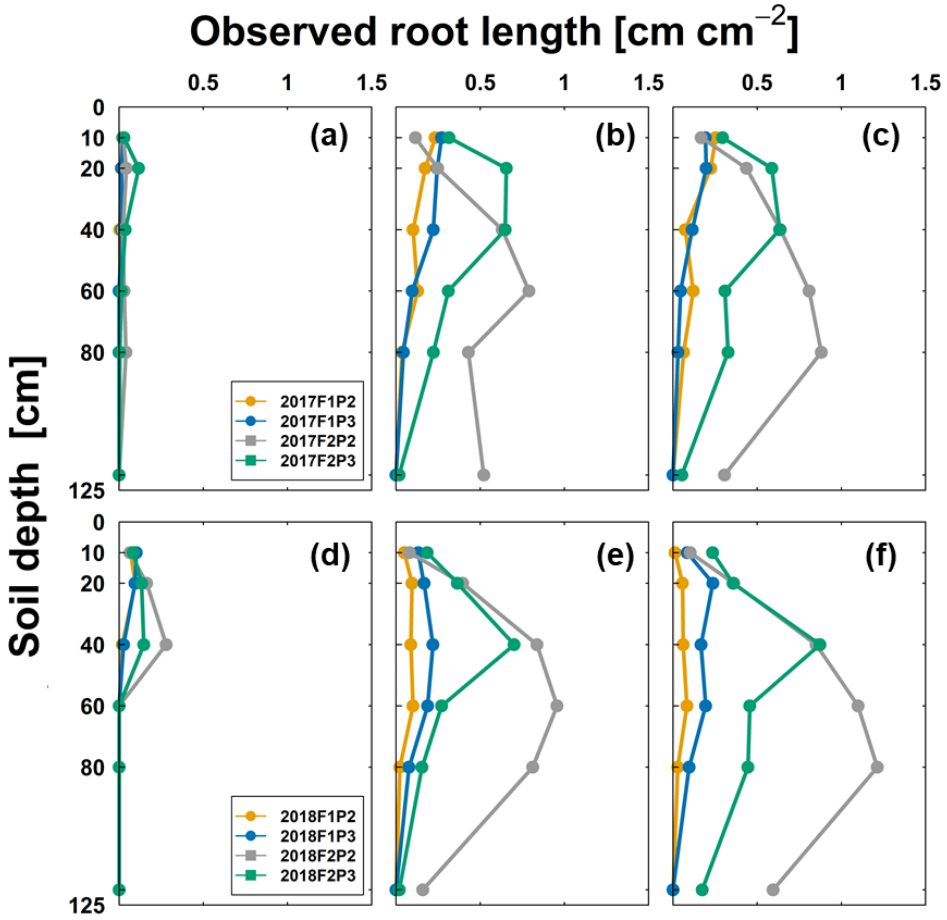
Observed root length [cm cm^{-2}]
0.5
1
1.5
Soil depth [cm]
0
10
20
40
60
80
125
(a)
(b)
(c)
(d)
(e)
(f)
2017F1P2
2017F1P3
2017F2P2
2017F2P3
2018F1P2
2018F1P3
2018F2P2
2018F2P3

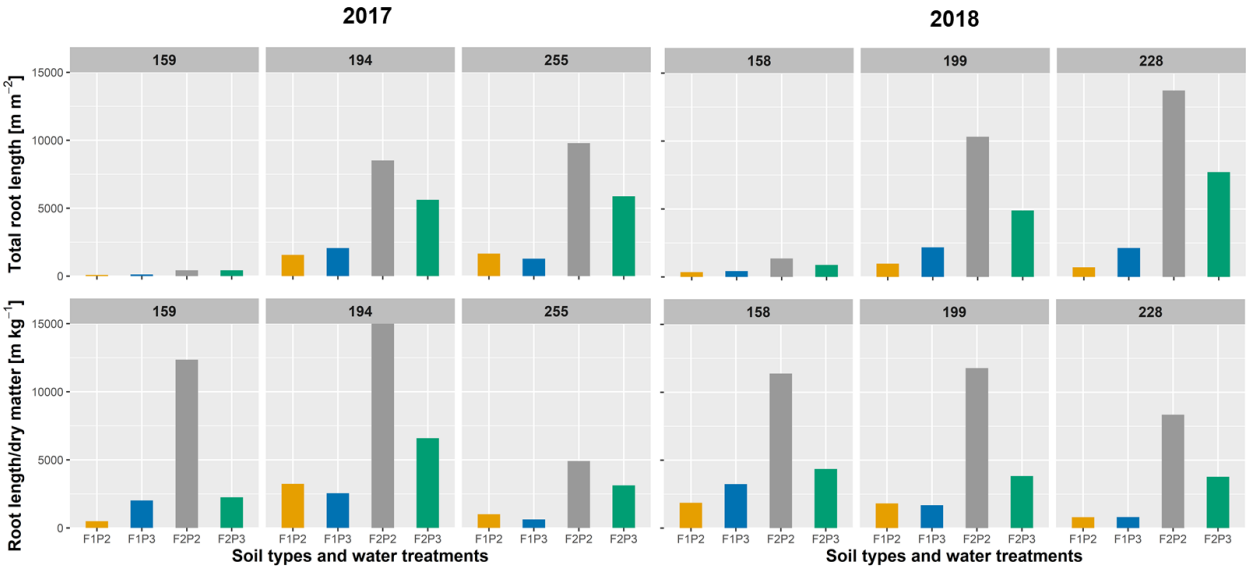
2017
2018
159
194
255
158
199
228
Total root length [m m^{-2}]
Root length/dry matter [m kg^{-1}]
0
5000
10000
15000
F1P2
F1P3
F2P2
F2P3
Soil types and water treatments

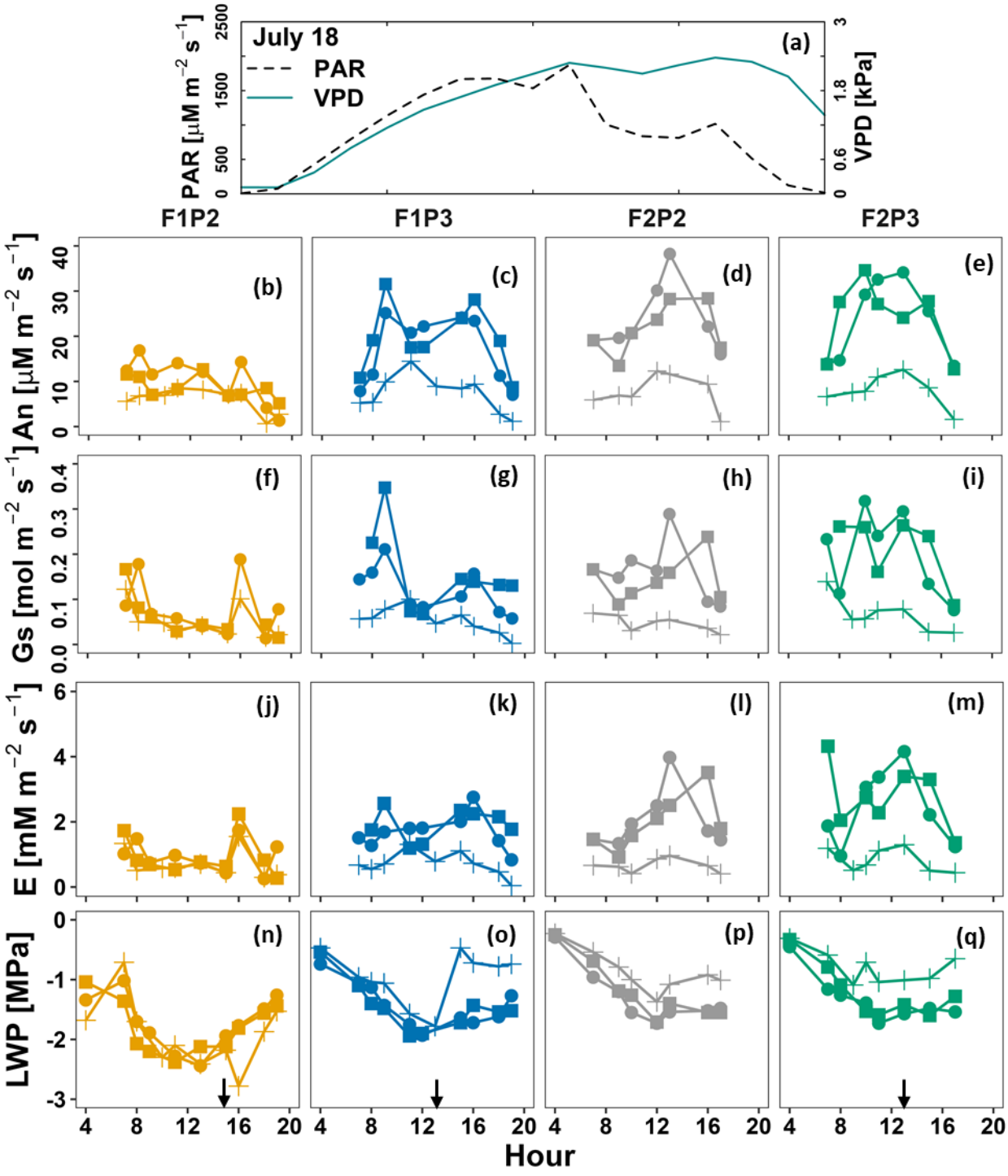
July 18
PAR
VPD
(a)
PAR [μM m^{-2} s^{-1}]
VPD [kPa]
F1P2
F1P3
F2P2
F2P3
(b)
(c)
(d)
(e)
An [μM m^{-2} s^{-1}]
(f)
(g)
(h)
(i)
Gs [mol m^{-2} s^{-1}]
(j)
(k)
(l)
(m)
E [mM m^{-2} s^{-1}]
(n)
(o)
(p)
(q)
LWP [MPa]
Hour

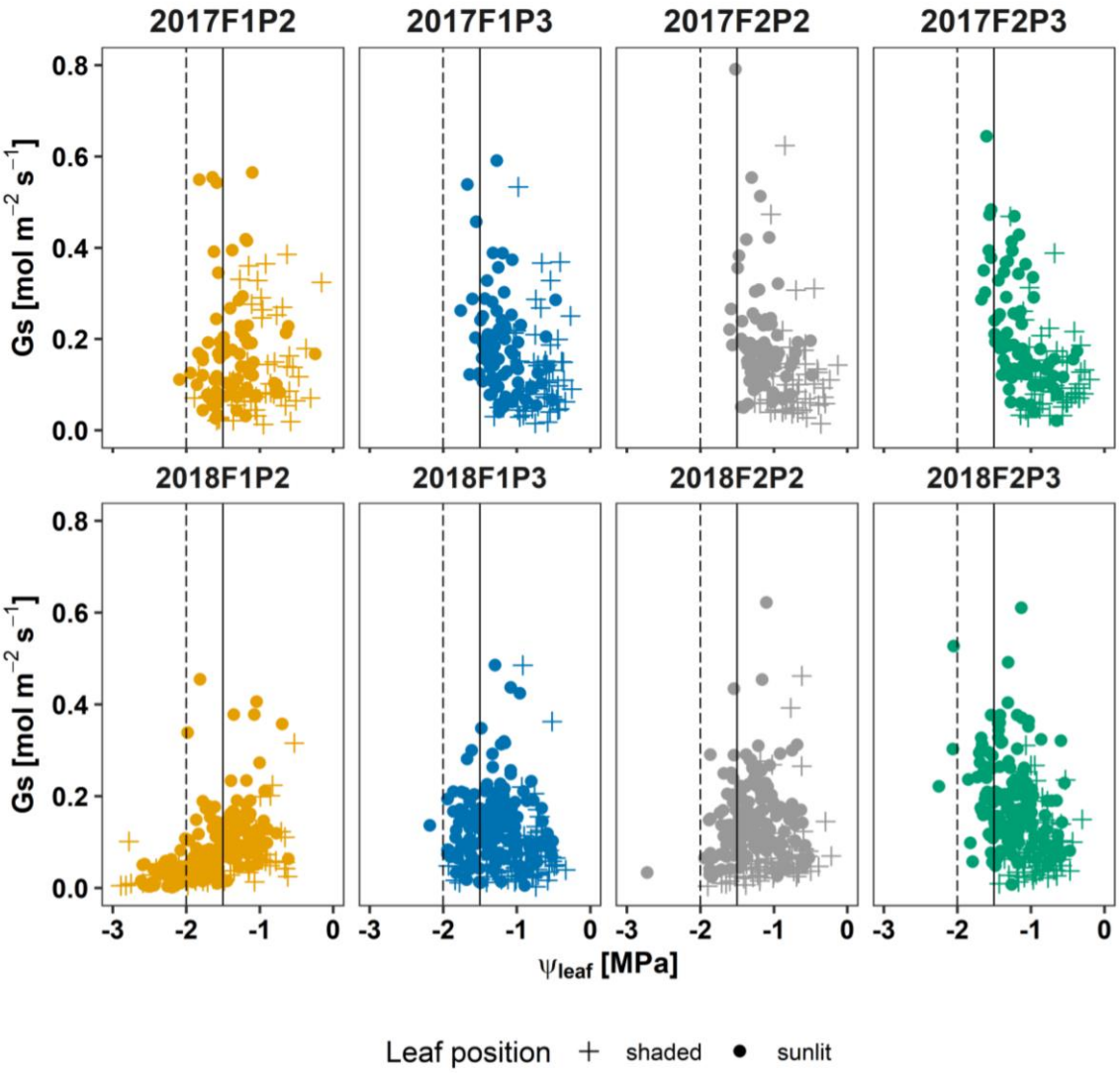
2017F1P2
2017F1P3
2017F2P2
2017F2P3
2018F1P2
2018F1P3
2018F2P2
2018F2P3
Gs [mol m^{-2} s^{-1}]
0.0
0.2
0.4
0.6
0.8
-3
-2
-1
0
Ψ_{leaf} [MPa]
Leaf position
shaded
sunlit

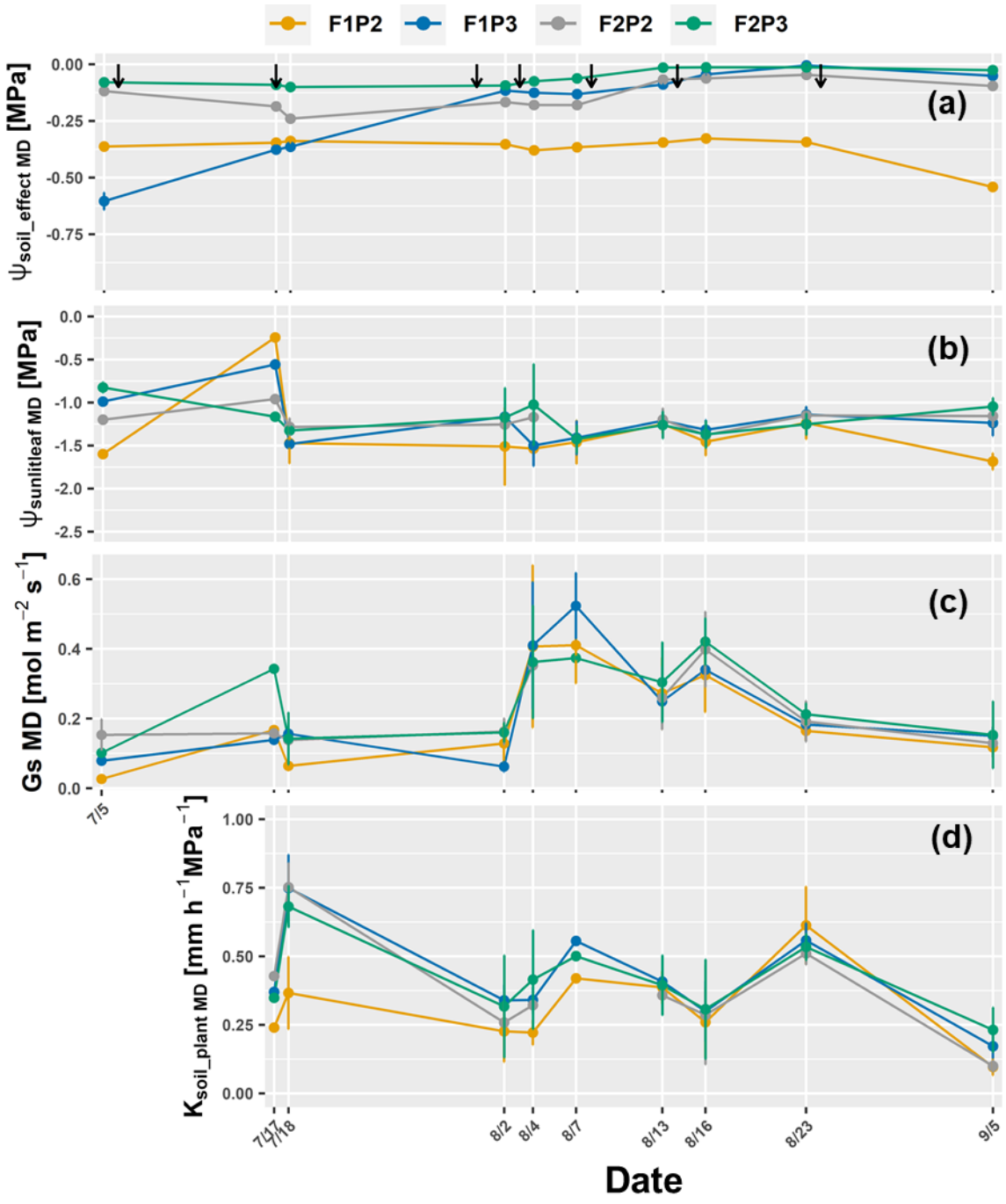
F1P2
F1P3
F2P2
F2P3
(a)
(b)
(c)
(d)
ψsoil_effect MD [MPa]
ψsunlitleaf MD [MPa]
Gs MD [mol m−2 s−1]
Ksoil_plant MD [mm h−1MPa−1]
0.00
-0.25
-0.50
-0.75
0.0
-0.5
-1.0
-1.5
-2.0
-2.5
0.6
0.4
0.2
0.0
1.00
0.75
0.50
0.25
0.00
7/5
7/17
7/18
8/2
8/4
8/7
8/13
8/16
8/23
9/5
Date

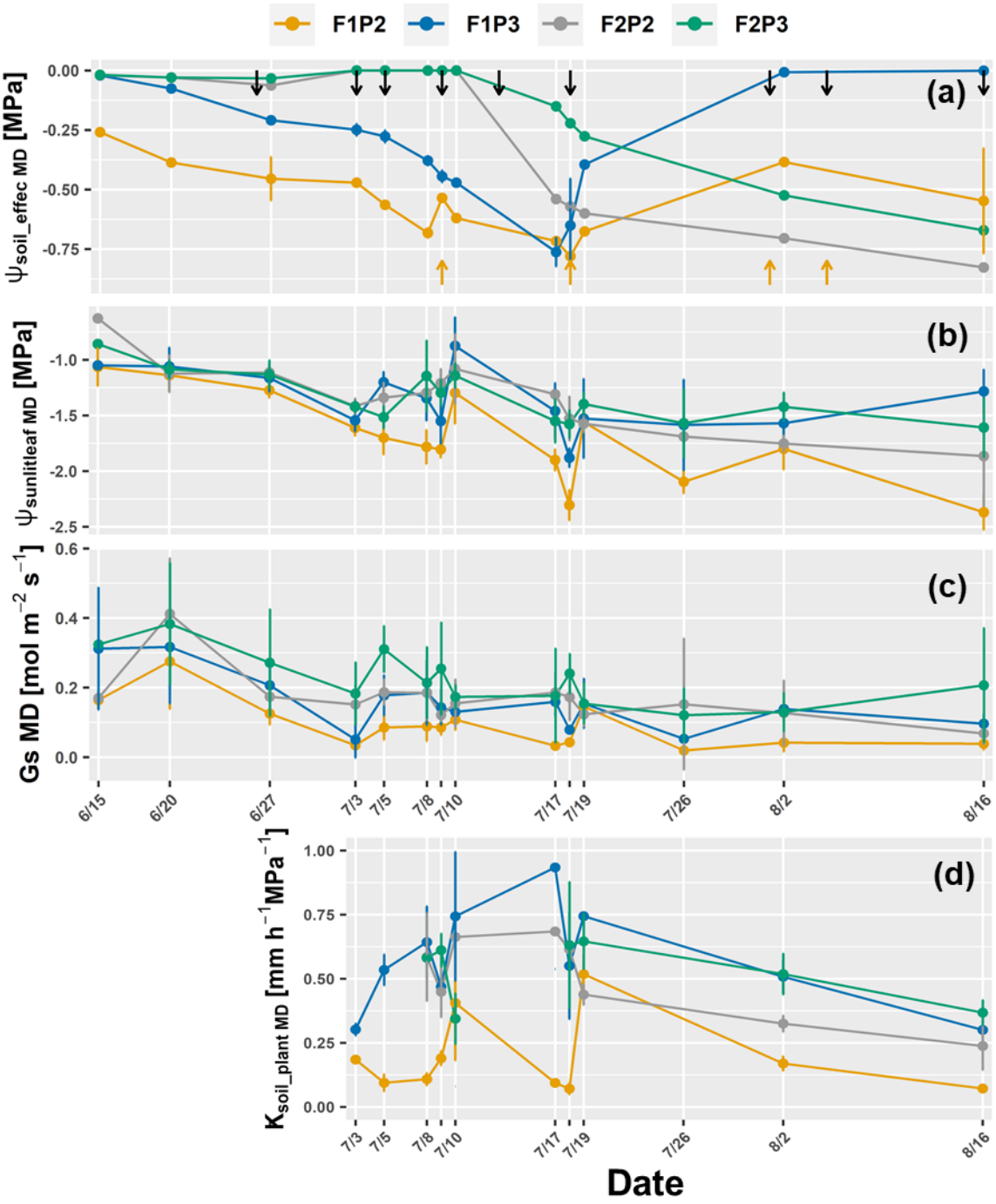
F1P2
F1P3
F2P2
F2P3
(a)
$\psi_{soil\_effec\ MD}$ [MPa]
0.00
-0.25
-0.50
-0.75
(b)
$\psi_{sunlitleaf\ MD}$ [MPa]
-1.0
-1.5
-2.0
-2.5
(c)
Gs MD [mol m^{-2} s^{-1}]
0.6
0.4
0.2
0.0
6/15
6/20
6/27
7/3
7/5
7/8
7/10
7/17
7/19
7/26
8/2
8/16
(d)
$K_{soil\_plant\ MD}$ [mm h^{-1}MPa^{-1}]
1.00
0.75
0.50
0.25
0.00
7/3
7/5
7/8
7/10
7/17
7/19
7/26
8/2
8/16
Date

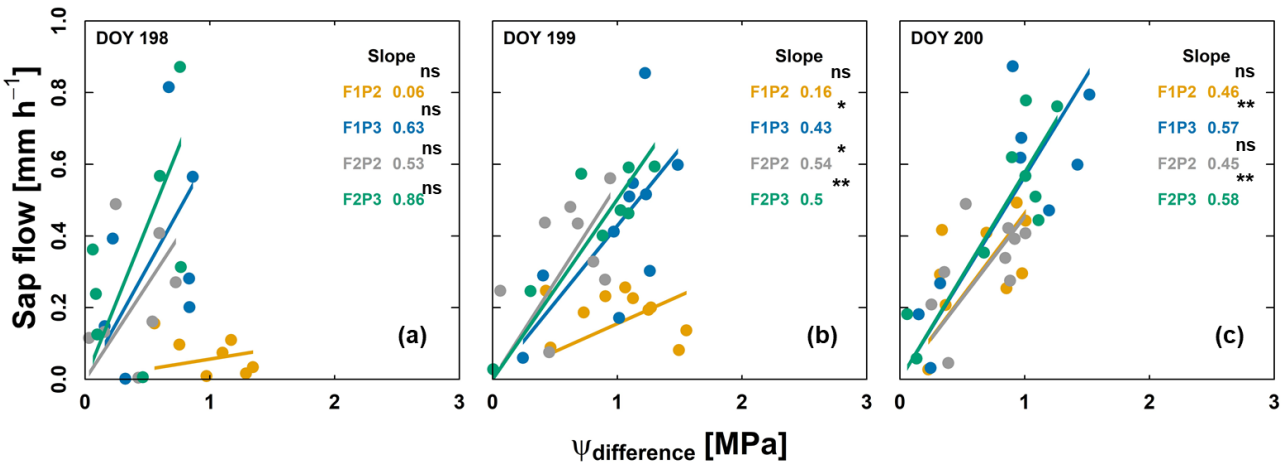
DOY 198
DOY 199
DOY 200
Slope
F1P2 0.06 ns
F1P3 0.63 ns
F2P2 0.53 ns
F2P3 0.86 ns
F1P2 0.16 *
F1P3 0.43 *
F2P2 0.54 **
F2P3 0.5 **
F1P2 0.46 **
F1P3 0.57 ns
F2P2 0.45 **
F2P3 0.58
(a)
(b)
(c)
Sap flow [mm h^{-1}]
$\Psi_{difference}$ [MPa]
0.0
0.2
0.4
0.6
0.8
1.0
0
1
2
3

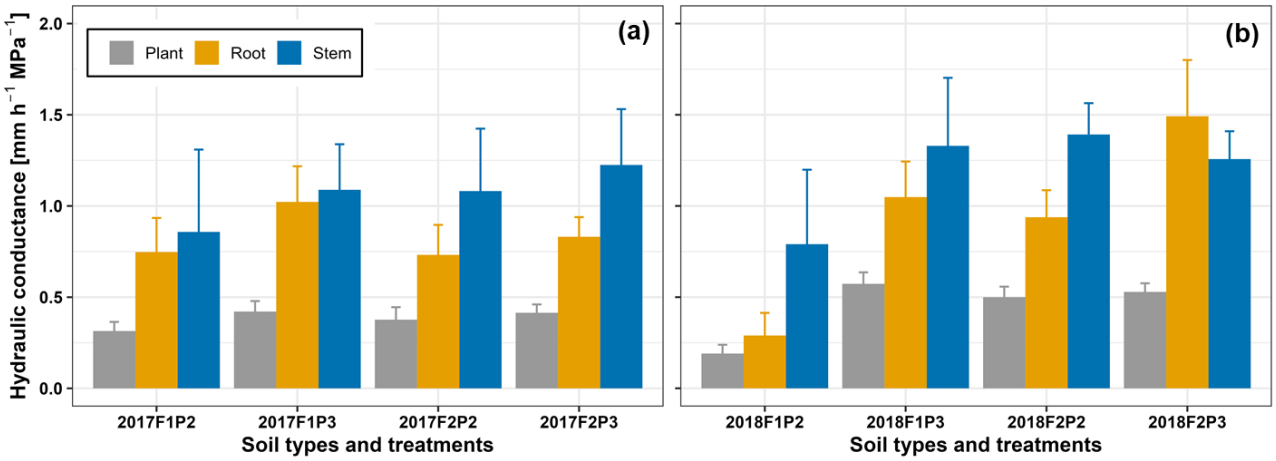
(a)
(b)
Plant
Root
Stem
Hydraulic conductance [mm h^{-1} MPa^{-1}]
2.0
1.5
1.0
0.5
0.0
2017F1P2
2017F1P3
2017F2P2
2017F2P3
2018F1P2
2018F1P3
2018F2P2
2018F2P3
Soil types and treatments
Soil types and treatments

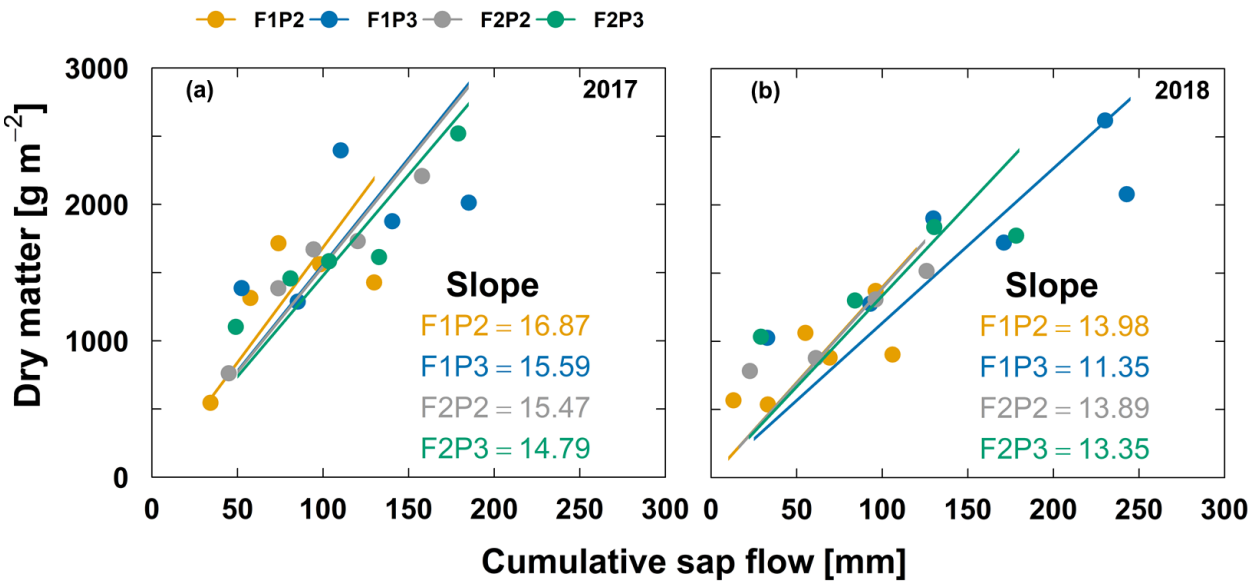
F1P2
F1P3
F2P2
F2P3
(a)
2017
(b)
2018
Dry matter [g m^{-2}]
Cumulative sap flow [mm]
Slope
F1P2 = 16.87
F1P3 = 15.59
F2P2 = 15.47
F2P3 = 14.79
Slope
F1P2 = 13.98
F1P3 = 11.35
F2P2 = 13.89
F2P3 = 13.35
0
1000
2000
3000
0
50
100
150
200
250
300